HHS Public Access

Author manuscript

Nat Cell Biol. Author manuscript; available in PMC 2022 July 13.

Published in final edited form as:

Nat Cell Biol. 2022 January ; 24(1): 74–87. doi:10.1038/s41556-021-00813-8.

The Hippo pathway kinases LATS1 and 2 attenuate cellular responses to heavy metals through phosphorylating MTF1

Han Han[1], **Hiroki J Nakaoka**[1], **Line Hofmann**[1], **Jeff Jiajing Zhou**[1], **Clinton Yu**[2], **Lisha Zeng**[3], **Junyu Nan**[3], **Gayoung Seo**[1], **Rebecca Elizabeth Vargas**[1], **Bing Yang**[1], **Ruxi Qi**[4], **Lee Bardwell**[1], **Dmitry A. Fishman**[5], **Ken W.Y. Cho**[1], **Lan Huang**[2], **Ray Luo**[3,6,7,8], **Rahul Warrior**[1,*], **Wenqi Wang**[1,*]

[1]Department of Developmental and Cell Biology, University of California, Irvine, Irvine, CA 92697, USA

[2]Department of Physiology and Biophysics, University of California, Irvine, Irvine, CA 92697, USA

[3]Department of Molecular Biology and Biochemistry, University of California, Irvine, Irvine, CA 92697, USA

[4]Cryo-EM Center, Southern University of Science and Technology, Shenzhen, 518055, China

[5]Department of Chemistry, University of California, Irvine, Irvine, CA 92697, USA

[6]Department of Chemical and Biomolecular Engineering, University of California, Irvine, Irvine, CA 92697, USA

[7]Department of Materials Science and Engineering, University of California, Irvine, Irvine, CA 92697, USA

[8]Department of Biomedical Engineering, University of California, Irvine, Irvine, CA 92697, USA

Abstract

Heavy metals are both integral parts of cells and environmental toxicants, whose deregulation is associated with severe cellular dysfunction and various diseases. Here, we show that the Hippo pathway plays a critical role in regulating heavy metal homeostasis. Hippo signaling deficiency promotes heavy metal response gene transcription and protects cells from heavy metal-induced toxicity, a process independent of its classic downstream effectors YAP and TAZ. Mechanistically, the Hippo pathway kinase LATS phosphorylates and inhibits MTF1, an essential transcription factor in heavy metal response, resulting in the loss of heavy metal response gene transcription and cellular protection. Moreover, LATS activity is inhibited upon heavy metal treatment, where accumulated zinc directly binds and inhibits LATS. Taken together, our study reveals an interplay

*Correspondence: rwarrior@uci.edu (R.W.) and wenqiw6@uci.edu (W.W.).

Author contributions

H.H. and W.W. conceived and designed the study; W.W. supervised the study; H.H. and H.J.N. performed all the experiments with the assistance from G.S., R.E.V. and B.Y.; L.H. and R.W. performed the *Drosophila* survival study; C.Y. and L.H. performed the mass spectrometry analysis; L.B. helped with the *in vitro* kinase assay; J.N., L.Z., Q.R. and R.L. performed the simulation analysis; J.J.Z and K.W.Y.C helped with the RNAseq analysis; D.A.F. helped with the CD analysis; W.W. wrote the manuscript.

Competing interests

The authors declare no competing interests.

between the Hippo pathway and heavy metals, providing insights into this growth-related pathway in tissue homeostasis and stress response.

Keywords

The Hippo pathway; LATS; MTF1; heavy metal response; zinc

Heavy metals comprise a number of essential and non-essential metals for human. Genetic variations in genes involved in heavy metal adsorption, distribution, metabolism and excretion, have been associated with many human diseases[1-3]. Upon heavy metal load, transcription of genes encoding metallothioneins (MTs), which play a crucial role in heavy metal metabolism and detoxification[4-8], and other proteins like heavy metal transporters is dramatically induced[1, 5, 9, 10]. This process is tightly controlled by metal regulatory transcription factor 1 (MTF1), a ubiquitously expressed transcription factor that binds the metal response element (MRE) within the promoters of heavy metal response genes[11, 12] and regulates their transcription[13, 14].

Zn directly binds MTF1 and triggers MTF1-mediated heavy metal response. Zn binding induces the nuclear translocation of MTF1[15] and facilitates a local DNA conformational change to maximize DNA-binding affinity for MTF1[16]. As for other heavy metals (e.g. Cd, Cu, Fe, Pb), they displace Zn from its protein storage (e.g. MTs) to increase cellular Zn level and indirectly activate MTF1[15].

Drosophila lacking *mtf1* is viable but extremely sensitive to heavy metal exposure[17]. Mice lacking *Mtf1* die at embryonic stage due to liver degeneration[18, 19]. Dysregulation of MTF1 is associated with many human diseases such as neurodegeneration and cancers[20-22]. These facts underscore a crucial role of MTF1 in both heavy metal stress response and normal physiology; however, detailed regulation of MTF1 has not been fully elucidated. Here, we report a regulation of MTF1 by the Hippo pathway in heavy metal response.

The Hippo pathway is a key signaling pathway that controls organ size and cancer in animals[23-28]. In the mammalian Hippo pathway, serine/threonine protein kinases MST1/2 together with their adaptor SAV1 phosphorylate and activate the serine/threonine protein kinases LATS1/2 as well as their adaptor MOB1. MAP4Ks[29-33] function in parallel to MST1/2 to similarly phosphorylate and activate LATS1/2. Although acting as upstream kinases of MST1/2[34, 35], TAOKs also phosphorylate and activate LATS1/2[36]. NF2 is a plasma membrane-associated component required for the Hippo pathway kinase cascade activation[37, 38]. Downstream of LATS1/2 are two transcriptional co-activators YAP and TAZ, which are phosphorylated by LATS1/2 and retained in the cytoplasm for degradation[25, 26, 39]. Inactivation of Hippo signaling promotes YAP/TAZ nuclear translocation, where they bind transcription factors like TEADs to induce transcription of genes involved in proliferation and survival[40-42].

In this study, we discovered a function of the Hippo pathway in regulating heavy metal response through MTF1 but not YAP and TAZ. LATS phosphorylates MTF1 at S152 and disrupts its association with the promoters of heavy metal response genes, resulting in the

loss of heavy metal response gene expression. The Hippo pathway is inhibited upon heavy metal treatment, where accumulated Zn directly binds LATS kinase domain and inhibits LATS kinase activity. Taken together, our study uncovers an important role of the Hippo pathway in heavy metal response and sheds light on the poorly characterized mechanism underlying heavy metal homeostasis.

Results

Inhibition of the Hippo pathway reduces heavy metal toxicity

We tested several “unfavorable” conditions for cell growth and found that the Hippo pathway played a role in heavy metal response. As shown in Fig. 1a,b, supplementing additional Na, K, Ca or Mg did not affect the viability of wild-type HEK293A and the LATS1/2 double knockout (DKO) cells; as for heavy metals, treatment with Ag, Mn, Cu or Fe did not result in viability difference between these cells. Interestingly, treatment with Cd or Zn dramatically induced wild-type cell death, but only had mild effect on the LATS1/2 DKO cells (Fig. 1a,b). These findings were further confirmed by treating cells with different doses of Cd and Zn, where the LATS1/2 DKO cells showed higher LC_{50} value (~80 μM for Cd and ~280 μM for Zn) than wild-type cells (~6 μM for Cd and ~170 μM for Zn) (Fig. 1c). As for other Hippo pathway components, the MOB1A/B DKO cells and NF2 KO cells also showed resistance to the Cd/Zn-induced toxicity (Fig. 1d,e). In contrast, the MST1/2 DKO cells, in which both LATS activity and YAP phosphorylation were not largely affected[31, 36, 43], were similarly sensitive to Cd/Zn treatment as compared to wild-type cells (Fig. 1d,e). These data suggest a negative role of the Hippo pathway in protecting cells from Cd/Zn-induced toxicity.

Interestingly, cells stably expressing YAP-5SA (a YAP-active mutant)[44] (Extended Data Fig. 1a) did not show resistance to Cd/Zn treatment (Fig. 1f, g). Although depletion of YAP and TAZ (Extended Data Fig. 1b) reduced the LATS1/2 DKO cell growth under normal condition, the LATS1/2 DKO cell viability was not dramatically inhibited as compared to that of the wild-type cells upon Cd/Zn treatment (Fig. 1h,i). These data indicate that YAP and TAZ are dispensable in the Hippo pathway-mediated cellular response to Cd and Zn.

The Hippo pathway controls heavy metal response genes

Both RNAseq and Gene Ontology (GO) analyses showed that the cell apoptosis-related genes were enriched in the Cd/Zn-treated wild-type cells, while genes involved in response to metal ions and ion detoxification were enriched in the Cd/Zn-treated LATS1/2 DKO cells (Fig. 2a). We revealed a group of 181 genes controlled by both heavy metals and LATS1/2 (Fig. 2b), and clustered them into four groups based on their relative expression (Fig. 2c and Supplementary Table 1). Among them, a set of 71 genes, which were highly enriched in the GO terms for ion response, ion detoxification and anti-apoptosis (Fig. 2d), were significantly elevated in the LATS1/2 DKO cells, including MT family genes *MT1B*, *MT1G*, *MT1F*, and Zn transporter *ZNT2* (i.e. *SLC30A2*) (Fig. 2c). This finding was confirmed by an independent q-PCR screen study among the heavy metal response-related *MT*, *ZNT* (i.e. *SLC30*) and *ZIP* (i.e. *SLC39*) gene families, where *MT1A*, *MT1H*, *MT2A* were identified as additional *MT* genes that were significantly upregulated in the Cd/Zn-treated LATS1/2

DKO cells (Fig. 2e and Extended Data Fig. 1c,d). Consistently, the transcription of *MT1A* and *ZNT2* was largely increased in the MOB1A/B DKO and NF2 KO cells (Fig. 2f,g). Similar findings were observed in the LATS1/2- and MOB1A/B-deficient MCF10 DCIS cells (Fig. 2h) and under the Hippo signaling-inactivating conditions (Extended Data Fig. 1e-h). Moreover, loss of LATS1/2 promoted the transcription of *MT1A* and *MT1F* upon both serum starvation (Extended Data Fig. 1i,j) and treatment of Zn with different anions (Extended Data Fig. 1k,l). Collectively, these results demonstrate that Hippo signaling deficiency promotes heavy metal response gene transcription.

Loss of YAP and TAZ did not affect the elevated expression of *MT1A* and *ZNT2* in the Cd/Zn-treated LATS1/2 DKO cells (Fig. 2i,j), although their downstream gene *CTGF* transcription was largely inhibited (Fig. 2k). Targeting the YAP/TAZ-TEAD complex formation by Verteporfin (VP) did not affect the elevated *MT1A* expression in the Cd/Zn-treated LATS1/2 DKO cells (Fig. 2l), but largely reduced *CTGF* expression (Fig. 2m). These data suggest that the Hippo pathway regulates heavy metal response gene transcription independent of YAP and TAZ.

The Hippo pathway regulates heavy metal response via MTF1

Interestingly, depletion of MTF1 (Fig. 3a) dramatically reduced the viability (Fig. 3b,c) and the transcription of heavy metal response genes for the Cd/Zn-treated LATS1/2 DKO cells (Fig. 3d-h). MRE luciferase reporter assay showed that MTF1's transcriptional activity was largely enhanced in the LATS1/2 DKO cells (Fig. 3i) but was significantly reduced when LATS1, but not its kinase dead (KR) mutant, was overexpressed (Fig. 3j). These data suggest that MTF1 is required for the Hippo pathway-mediated heavy metal response and its transcriptional activity is inhibited by LATS.

Overexpression of TEAD4 did not affect the MTF1's transcriptional activity (Fig. 3j), while loss of MTF1 did not affect the elevated expression of *CTGF* and *CYR61* in the LATS1/2 DKO cells (Fig. 3k). These results indicate that MTF1 and the YAP/TAZ-TEAD complex regulate independent transcription programs downstream of the Hippo pathway.

Loss of LATS promotes the association of MTF1 with DNA

MTF1 was majorly localized in the cytoplasm of the LATS1/2 DKO cells under normal condition but translocated into the nucleus upon Cd/Zn treatment (Fig. 3l,m), suggesting that LATS did not regulate its cellular localization. To overcome the antibody issue, we used inducible lentiviral system to make the expression of SFB-tagged MTF1 close to that of endogenous MTF1 (Extended Data Fig. 1m), and subjected the stable cells to a chromatin immunoprecipitation (ChIP) assay. As shown in Fig. 3n, Cd/Zn-induced binding of MTF1 to the promoters of heavy metal response genes *MT1F* and *ZNT2* was largely enhanced in the LATS1/2 DKO cells, indicating that LATS inhibits the association of MTF1 with heavy metal response genes' promoters.

Loss of MTF1 did not change YAP nuclear localization in the LATS1/2 DKO cells (Fig. 3l,m), and expression of YAP-5SA mutant did not affect MTF1's association with heavy metal genes' promoters (Fig. 3n and Extended Data Fig. 1m), consistently showing an independent relationship between MTF1 and YAP.

LATS1 binds and phosphorylates MTF1 at S152

Exogenously expressed SFB-MTF1, whose expression was made close to endogenous MTF1, formed a complex with LATS1 (Extended Data Fig. 2a). Additionally, MTF1 specifically interacted with LATS1 among the tested Hippo pathway components (Fig. 4a and Extended Data Fig. 2b). Because LATS1 kinase activity was required to inhibit MTF1 (Fig. 3j), we examined whether LATS1 could phosphorylate MTF1. A series of MTF1 truncation proteins (Fig. 4b) were purified from bacteria and subjected to the LATS1 *in vitro* kinase assay (Fig. 4c). Among them, the MTF1-R2 region was found to be phosphorylated by LATS1 (Fig. 4c). As a control, LATS1 kinase dead (KR) mutant failed to phosphorylate MTF1-R2 region (Extended Data Fig. 2c). Mass spectrometry analysis revealed six residues as potential LATS1 phosphorylation sites on MTF1-R2 region (Fig. 4d), where the S152 and S305 sites were phosphorylated *in vivo* (https://www.phosphosite.org/) (Fig. 4d). As for these identified sites, the S305A mutation did not affect the LATS1-mediated phosphorylation of MTF1-R2 region (Fig. 4e), while mutating the remaining five residues (the 5A mutant: S152A/T153A/T241A/S301A/T302A) dramatically abolished it (Fig. 4e and Extended Data Fig. 2c). Further characterization of these five residues showed that LATS1 phosphorylated MTF1-R2 region at S152/T153 (Fig. 4e). We reversely mutated each residue(s) back to wild-type for the MTF1-5A mutant, and eventually revealed S152 as the LATS1 phosphorylation site on MTF1 (Fig. 4f). This finding was confirmed using a phospho-antibody against p-MTF1 S152 both *in vitro* (Fig. 4g) and *in vivo* (Fig. 4h). MTF1 S152 phosphorylation was dramatically reduced in the LATS1/2 DKO cells (Fig. 4h), while overexpression of LATS1 but not its kinase dead (KR) mutant enhanced it (Extended Data Fig. 2d). As controls, another two NDR family kinases STK38 and STK38L failed to phosphorylate MTF1 at S152 (Extended Data Fig. 2e). These results together show that LATS1 binds and phosphorylates MTF1 at S152.

It is known that LATS phosphorylates its substrates containing a consensus phosphorylation motif (HxRxxS/T), where “x” could be any amino acid[44, 45]. However, the MTF1 S152-containing amino acid sequence (CxRxxS), which is highly conserved among different species (Fig. 4i), does not fit this pattern. We examined the H122C mutation for the YAP S127-containing motif, and found that YAP H122C mutant, but not its H122A mutant, was still phosphorylated at S127 (Fig. 4j). Whether additional proteins containing such “CxRxxS” motif can be phosphorylated by LATS deserves further investigation.

S152 phosphorylation inhibits MTF1 and heavy metal response

Interestingly, the S152A mutation significantly increased the MTF1-induced MRE luciferase activity, while the S152D mutation inhibited it (Fig. 5a,b). Overexpression of LATS1 largely attenuated the MTF1-induced MRE luciferase activity to the level induced by MTF1 S152D mutant (Fig. 5a,b). MTF1 S152 phosphorylation did not affect the Cd/Zn-induced MTF1 nuclear translocation (Fig. 5c). We generated the LATS/MTF1 triple KO (TKO) cells stably expressing the inducible SFB-tagged MTF1 and its S152D mutant, made their expressions close to that of endogenous MTF1 in wild-type cells (Fig. 5d), and subjected these reconstituted cells to a ChIP assay. As shown in Fig. 5e, the S152D mutation largely reduced the association of MTF1 with the promoters of heavy metal response genes *MT1F*

and *ZNT2* under Cd/Zn-treated conditions. These findings suggest that LATS-induced S152 phosphorylation inhibits MTF1 to bind heavy metal response genes' promoters.

Reconstituting MTF1, but not its S152D mutant, significantly rescued Cd/Zn-treated LATS/MTF1 TKO cell viability (Fig. 5f,g). Expression of MTF1, but not its S152D mutant, restored the transcription of *MT1A*, *MT1F* and *ZNT2* in the LATS/MTF1 TKO cells (Fig. 5h-j). Similar rescue experiments were performed in the MTF1 KO cells, where Cd/Zn-induced heavy metal response gene transcription was also abolished (Extended Data Fig. 3a,b). We generated the MTF1 KO cells stably expressing inducible SFB-tagged MTF1 and its S152A/S152D mutants, and made their expressions close to that of endogenous MTF1 in wild-type cells (Extended Data Fig. 3c). As shown in Extended Data Fig. 3d,e, reconstituting MTF1 S152A mutant, but not MTF1 or its S152D mutant, largely rescued MTF1 KO cell viability under Cd/Zn-treated conditions. Re-expressing MTF1 S152A mutant also significantly increased the transcription of heavy metal response genes *MTF1A* and *MT1F* in the Cd/Zn-treated MTF1 KO cells, while reconstitution of its S152D mutant failed to do so (Extended Data Fig. 3f,g). These results demonstrate that LATS-mediated S152 phosphorylation inhibits MTF1's transcriptional activity and heavy metal response.

It is unclear how the S152 phosphorylation diminishes MTF1's DNA binding due to the lack of MTF1 protein structure information. Alternatively, we examined the zinc finger domain (i.e. ZNF1) structure of ZAP1[46], the MTF1-like zinc-responsive transcriptional regulator in yeast, and found that this site (i.e. the S591 site of ZAP1) is adjacent to the first α-helix of ZNF1 (Extended Data Fig. 3h). Simulation analyses showed that both the S591 phosphorylation and phosphomimetic S591D mutation did not affect its Zn binding or cause a significant structure change (Extended Data Fig. 3h). Since zinc fingers are required for MTF1 DNA binding[1], we speculate that the S152 phosphorylation might affect the contact between MTF1 and DNA. Moreover, when MTF1 and its S152A/S152D mutants were translocated into the nucleus upon Zn treatment (Extended Data Fig. 3i), we failed to detect their interaction with the reported transcriptional regulators SP1[47], p300/CBP[47] and C/EBPα[48] for MTF1 (Extended Data Fig. 3j).

Targeting Hippo signaling drives heavy metal detoxification

Treatment with XMU-MP-1, a potent Hippo pathway inhibitor[49], significantly inhibited the phosphorylation of MOB1, LATS1 and YAP in Hep3B cells (Fig. 6a). XMU-MP-1 also protected cell viability (Fig. 6b,c) and enhanced the transcription of *MT1A* and *MT1F* under Cd/Zn-treated conditions (Fig. 6d). We also intoxicated mice with CdCl2 and treated them with XMU-MP-1 (Fig. 6e). XMU-MP-1 treatment significantly increased mouse overall survival (Fig. 6f and Supplementary Video 1,2), while combined treatment with Verteporfin (VP) did not affect the therapeutic role of XMU-MP-1 against CdCl2-induced toxicity (Fig. 6f and Supplementary Video 1,2). We examined the mouse liver and kidney tissues, but did not find obvious structure/morphology difference compared to the vehicle-treated mouse tissues (Fig. 6g). Interestingly, XMU-MP-1 treatment significantly induced Mtf1's nuclear translocation (Extended Data Fig. 4a), inhibited Mtf1 S151 phosphorylation (Extended Data Fig. 4a), increased metallothionein 1 (Mt1) protein expression (Fig. 6g), and reduced cell apoptosis (Fig. 6g) in the CdCl2-treated mouse liver and kidney tissues. Consistently, the

transcription of heavy metal response genes *Mt1* and *Mt2* was largely enhanced by XMU-MP-1 in the CdCl2-treated mouse liver and kidney tissues (Fig. 6h,i). Although combined treatment with VP dramatically reduced the expression of YAP/TAZ downstream gene *Ctgf* (Fig. 6h,i), it did not affect the XMU-MP-1-induced heavy metal response gene expression in the same tissues (Fig. 6g-i). Collectively, these data suggest the Hippo pathway as a therapeutic target for heavy metal detoxification.

As a MST1/2 inhibitor, XMU-MP-1 treatment enhanced heavy metal response in Hep3B cells (Fig. 6b-d), which was inconsistent with the findings observed in the MST1/2 DKO HEK293A cells (Fig. 1d,e and Fig. 2f,g). Although XMU-MP-1 treatment inhibited MST (as indicated by the reduced MOB1 T35 phosphorylation) in both Hep3B and HEK293A cells, it suppressed YAP S127 phosphorylation in Hep3B cells but not in HEK293A cells (Extended Data Fig. 4b). Consistently, YAP S127 phosphorylation was largely reduced in the MST1/2 DKO Hep3B cells but not in the MST1/2 DKO HEK293A cells (Extended Data Fig. 4b). Moreover, XMU-MP-1 treatment further enhanced the transcription of heavy metal response gene *MT1F* in the Cd/Zn-treated Hep3B cells (Extended Data Fig. 4c) but not HEK293A cells (Extended Data Fig. 4d). Therefore, MST kinase may play a dominant role in regulating LATS and heavy metal response in Hep3B cells, while its redundant kinases like MAP4Ks and TAOKs could majorly modulate these events in HEK293A cells. In addition, as compared to knockout of MST1/2, acute inhibition of MST by XMU-MP-1 showed more dramatic effects on YAP S127 phosphorylation (Extended Data Fig. 4b) and *MT1F* transcription (Extended Data Fig. 4c) in Hep3B cells, suggesting that adaptive response could be developed to compensate for LATS activation in the MST1/2 DKO Hep3B cells. Moreover, XMU-MP-1 treatment further inhibited YAP S127 phosphorylation (Extended Data Fig. 4b) and enhanced *MT1F* transcription (Extended Data Fig. 4c) in the MST1/2 DKO Hep3B cells, suggesting that XMU-MP-1 may regulate LATS and heavy metal response through other targets. Indeed, XMU-MP-1 treatment inhibited the ability of TAOK1 to phosphorylate LATS1 hydrophobic motif at T1079 (Extended Data Fig. 4e), but did not affect that of MAP4K2/4/6 kinases (Extended Data Fig. 4f-h), which is consistent with the finding in a previous study[49]. Notably, although XMU-MP-1 and knockout of MST1/2 show different effects on LATS and heavy metal response in different cells, LATS inhibition is consistently associated with the elevated heavy metal response, further confirming the negative role of LATS in regulating heavy metal response.

Hippo signaling controls heavy metal response in Drosophila

The MTF1 S152 site is conserved in different species including *Drosophila* (i.e. the S126 site of *Drosophila mtf1*) (Fig. 4i). *Drosophila mtf1* contains an extra cysteine-rich cluster for Cu sensing, allowing intracellular Cu to bind and activate *mtf1*[1, 50]. Therefore, Cu is also used to investigate the *mtf1*-dependent heavy metal response in *Drosophila*[17, 51]. Interestingly, *mats* heterozygous mutant *Drosophila* showed greater resistance to food containing high concentrations of heavy metals (e.g. 5 mM CuSO4) as compared to wild-type *Drosophila* and *mtf1* homozygous mutant (Extended Data Fig. 5a). Re-expressing *Drosophila mtf1* in the MTF1 KO HEK293A cells (Extended Data Fig. 5b) was able to rescue *MT1A* expression (Extended Data Fig. 5b,c). Moreover, the S126D mutation did not affect the Cd/Zn-induced *Drosophila mtf1* nuclear translocation (Extended Data Fig. 5d),

but disrupted its ability to rescue *MT1A* expression in the Cd/Zn/Cu-treated LATS/MTF1 TKO cells (Extended Data Fig. 5e,f). These findings indicate an evolutionarily conserved regulation of MTF1 and heavy metal response by the Hippo pathway.

The Hippo pathway is inhibited by heavy metals

Because YAP was translocated into the nucleus of Cd/Zn-treated HEK293A cells (Fig. 3l,m) and the transcription of *Ctgf* was induced in the CdCl2-treated mouse liver and kidney tissues (Fig. 6h,i), the Hippo pathway could be inhibited by heavy metals. Despite a dispensable role of YAP in the Hippo pathway-mediated heavy metal response, YAP is still a good readout for the Hippo pathway activity.

Among all the tested metals, Cd/Zn treatment largely reduced YAP S127 phosphorylation in Hep3B cells (Fig. 7a) and in a time-dependent manner (Extended Data Fig. 6a). Cd/Zn treatment induced YAP nuclear translocation (Fig. 7b) and the transcription of *CTGF* and *CYR61* (Fig. 7c) in Hep3B cells. Similar findings were observed in other cell lines including HEK293A, MCF10A and HeLa (Fig. 3l,7c and Extended Data Fig. 6b,c). Moreover, the expression and nuclear localization of Yap (Fig. 7d) as well as its downstream gene transcription (Fig. 7e) were significantly increased in the CdCl2-treated mouse liver and kidney tissues. MTF1 S152 phosphorylation was also reduced upon Cd/Zn treatment (Fig. 7f and Extended Data Fig. 4a,6d). Collectively, these data suggest that Cd/Zn treatment inhibits the Hippo pathway.

Indeed, LATS1 auto-phosphorylation at S909 (Extended Data Fig. 6e) and its hydrophobic motif phosphorylation at T1079 (Fig. 7g) were both decreased under Cd/Zn-treated conditions. In contrast, Cd/Zn treatment did not affect MST activity as indicated by the unchanged phosphorylation of MST and its substrate MOB1 (Fig. 7g). We also immunoprecipitated endogenous LATS1, MST1 and MAP4K4 from the Cd/Zn-treated Hep3B cells, and subjected them to *in vitro* kinase assay, where bacterially purified GST-YAP/MBP-MTF1-R2 (Fig. 4b) and MBP-LATS1-$C3^{52}$ proteins were used as substrates for LATS1 and MST1/MAP4K4, respectively. Consistently, Cd/Zn treatment strongly inhibited LATS1 as shown by the reduced phosphorylation of GST-YAP at S127 (Fig. 7h) and MBP-MTF1-R2 at S152 (Fig. 7i). In contrast, MST1 and MAP4K4 activities were not affected as indicated by the unchanged phosphorylation of MBP-LATS1-C3 at T1079 (Fig. 7j,k). Similarly, MAP4K2 and MAP4K6 were not affected by Cd/Zn (Fig. 7l,m). These data demonstrate that Cd/Zn treatment inhibits LATS but not MST or MAP4Ks.

Actually, all the tested tissues from the CdCl2-treated mice showed enhanced expression of *Mt1* (Extended Data Fig. 6f) and *Ctgf* (Extended Data Fig. 6g). Moreover, both *MTF1* and *LATS1* were expressed in different human tissues (Extended Data Fig. 6h), cells (Extended Data Fig. 6i) and commonly used cell lines (Extended Data Fig. 6j). These data indicate that the LATS-MTF1 axis may act in various types of cells and tissues to regulate heavy metal response.

Zn directly binds LATS

Because Cd/Zn treatment reduced LATS1 T1079 phosphorylation without affecting MST and MAP4Ks (Fig. 7g-m), we hypothesized that the access of MST/MAP4Ks to the

LATS1 T1079-containing region could be affected by Cd/Zn. Unexpectedly, we found that among all the tested metals (Extended Data Fig. 7a), Cu and Zn specifically interacted with LATS1/2 (Fig. 8a,b). As for the Hippo pathway components, Zn specifically bound LATS (Fig. 8c), while the association between Cu and Hippo pathway components were non-specific (Extended Data Fig. 7b). Treatment with the Zn chelator TPEN reduced the interaction between Zn and LATS1/2 (Extended Data Fig. 7c,d). We truncated LATS1 into *N*-terminal half and *C*-terminal half (Fig. 8d), and subjected them to the pulldown assay using Zn beads. As shown in Fig. 8e, Zn interacted with *C*-terminal half of LATS1. We further generated a series of truncations for the LATS1 *C*-terminal region (Fig. 8d) and purified them from bacteria. As shown in Fig. 8f, Zn directly bound LATS1-C3 protein, which contains the LATS1 hydrophobic motif (Fig. 8d).

Zn binding exerts dual inhibitory effects on LATS

Interestingly, chelating Zn by TPEN in the MST1 *in vitro* kinase assay increased the phosphorylation of MBP-LATS1-C3 at T1079, but did not affect MST1 auto-phosphorylation at T183 (Fig. 8g). On the other hand, supplementing Zn, but not control metal Ca, reduced the phosphorylation of MBP-LATS1-C3 at T1079 (Fig. 8h and Extended Data Fig. 7e,f). A similar finding was observed in the MAP4K2 *in vitro* kinase assay (Fig. 8h and Extended Data Fig. 7g). As a control, supplementing Zn did not affect MST1-induced phosphorylation of GST-MOB1 at T35 (Extended Data Fig. 7h). Moreover, treatment with Zn did not affect the association between LATS1 and its phosphatases PP1A (Extended Data Fig. 7i) and POPX2 (Extended Data Fig. 7j) known to target LATS1 T1079 phosphorylation[53, 54]. Since Zn did not bind MST1 or MAP4K2 (Fig. 8c) and Zn treatment did not affect their auto-phosphorylation (Extended Data Fig. 7f,g), these results suggest that Zn binding to LATS1-C3 region inhibited the MST1/MAP4K2-induced LATS1 T1079 phosphorylation.

Additionally, chelating Zn in the LATS1 *in vitro* kinase assay increased GST-YAP phosphorylation at S127 (Fig. 8i), while supplementing Zn, but not control metal Ca, inhibited it (Fig. 8j and Extended Data Fig.7k,l). Similar finding was observed in the LATS2 *in vitro* kinase assay (Fig. 8j and Extended Data Fig. 7m). As for these experiments, Zn binding did not affect the T1079/T1041 phosphorylation for LATS1/2 that were purified from HEK293T cells (Extended Data Fig. 7l,m). These data suggest that Zn binding also inhibits LATS intrinsic kinase activity.

To determine whether Zn binding may cause the conformational change for LATS1-C3 region, we subjected the bacterially purified MBP-LATS1-C3 protein (Fig. 8k) to circular dichroism (CD) analysis. Interestingly, supplementing Zn, but not Ca, altered the MBP-LATS1-C3 protein structure in a dose-dependent manner (Fig. 8l,m). As a control, MBP protein structure was not affected by Zn under the same experimental setting (Fig. 8n). Collectively, these results show that Zn binding disturbs the LATS1-C3 protein structure, which may affect LATS hydrophobic motif phosphorylation and its intrinsic kinase activity.

The Hippo-MTF1 axis acts in response to other heavy metals

Since Cd treatment strongly inhibited LATS (Fig. 7g-i), we examined whether Cd could regulate other Hippo pathway components. Indeed, Cd treatment attenuated the association between LATS1 and MOB1, while Zn treatment did not affect it (Extended Data Fig. 8a). Moreover, Cd did not bind LATS (Fig. 8a,b) or MOB1 (Extended Data Fig. 8b). These findings suggest that Cd targets the LATS1-MOB1 complex formation through a yet-to-be identified mechanism. Cu treatment only partially reduced YAP phosphorylation at S127 (Fig. 7a) and weakly increased the transcription of heavy metal response genes *MT1A* and *MT1F* and YAP downstream gene *CYR61* (Extended Data Fig. 8c). Loss of LATS1/2 further enhanced the Cu-induced transcription of *MT1A* (Extended Data Fig. 8d), suggesting that the Hippo pathway also controls the Cu-induced heavy metal response. Chelating Cu by tetrathiomolybdate (TTM) did not affect the ability of LATS1 to phosphorylate GST-YAP at S127 (Extended Data Fig. 8e), suggesting that Cu dose not directly regulate LATS.

Cisplatin and carboplatin are both platinum-based compounds (Extended Data Fig. 8f), which have been widely used in chemotherapy[55]. Treatment with cisplatin and carboplatin also induced the transcription of heavy metal response gene *MT1A* (Extended Data Fig. 8g). Loss of LATS1/2 further enhanced cisplatin/carboplatin-induced *MT1A* expression, while depletion of MTF1 abolished it (Extended Data Fig. 8g). Furthermore, a positive correlation between the expressions of the YAP/TAZ downstream genes (e.g. *CTGF*, *CYR61*, *ANKRD1*) and heavy metal response genes (e.g. *MT1A*, *MT2A*) was identified in the cisplatin/carboplatin-treated lung squamous cell carcinoma (LUSC) samples in The Cancer Genome Atlas (TCGA) (Extended Data Fig. 8h,i). Since we did not detect a significant correlation between the expressions of *YAP1*/*WWTR1* and heavy metal response genes (e.g. *MT1A*, *MT2A*) in the same patient samples (Extended Data Fig. 8j,k), the elevated heavy metal response could be caused by Hippo signaling inactivation. These findings together implicate a clinical relevance of the Hippo pathway-mediated heavy metal response in platinum-based chemotherapy.

Discussion

Different from previously reported kinases such as ATM, PKC, JNK, PI3K, CKII, tyrosine-specific protein kinases that indirectly modulated MTF1[56, 57], our study revealed LATS as a kinase of MTF1 inhibiting its transcriptional activity. Because MTF1 did not affect YAP/TAZ's cellular localization or transcriptional activities (Fig. 3k-m), the MTF1-dependent heavy metal response may not be involved in the Hippo pathway-mediated organ size control.

We hardly observed any obvious growth and survival defects for the cells with MTF1 deficiency or expressing its S152A and S152D mutants under normal condition. However, upon heavy metal exposure, this "silent" phosphorylation turns out to become a key regulatory event for heavy metal response and cell viability. Thus, the Hippo pathway-mediated heavy metal response could be an inadvertent consequence, which is similar to the *haly-1* deficiency-induced heavy metal resistance in *C. elegans*[58]. Since MTF1 plays important roles in normal physiology[18, 19] and its dysregulation is associated with many human diseases[20-22], the Hippo pathway may play a yet-to-be defined role in the

MTF1-related physiological events. Notably, our data connected the Hippo-MTF1 pathway to platinum-based chemotherapy (Extended Data Fig. 8f-k), underscoring its clinical significance.

MTF1 and *LATS1* are both widely expressed in different human tissues/cells (Extended Data Fig. 6h-j). Regulation of MTF1 and heavy metal response by the Hippo pathway were observed in *Drosophila* (Extended Data Fig. 5), mice (Fig. 6g-i and Extended Data Fig. 6f,g) and cancer patient samples (Extended Data Fig. 8h-k). These facts suggest that the Hippo-MTF1 pathway acts in various types of cells, tissues and animals.

Here, we majorly used Zn and Cd to activate MTF1 and heavy metal response. Importing Zn into cells is mediated by human ZIP (SLC39) transporter family comprising 14 members, among which 9 are localized on the plasma to drive Zn entry[59]. Cd can also be imported through a variety of ion transporters[60]. These facts suggest that many transporters are available to for Zn and Cd. Although other heavy metals like Cu and Fe can indirectly activate MTF1 through Zn[15], their mild effects on cell viability (Fig. 1a,b) and the Hippo pathway (Fig. 7a) could be caused by their limited cell entry[61-63]. Moreover, Zn exerted a threshold-sensitive effect on cell viability, while Cd targeted it in a dose-dependent manner (Fig. 1c). This discrepancy could be explained by the facts that Zn is an essential heavy metal for humans as structural, catalytic and cellular signaling component; therefore, low amount of Zn could be incorporated into its cellular complexes for storage and neutralization, resulting in a threshold-sensitive effect on cell viability. In contrast, Cd is a non-essential heavy metal with extremely high toxicity, making its effect on cell viability dose-dependent.

Our study also reveals a regulation of the Hippo pathway by heavy metals (Fig. 7 and 8). Upon heavy metal load, elevated Zn binds MTF1 to induce its nuclear localization; meanwhile, Zn binds and inhibits LATS to promote MTF1 DNA binding (Extended Data Fig. 8l). Since heavy metals like Cd, Cu, Fe, Pb, can indirectly induce Zn release from its cellular protein storage to activate MTF1 and heavy metal response[1, 64], similar mechanism could be utilized by other heavy metals to target LATS. However, we cannot rule out the possibility that ions may modulate LATS via other mechanisms. For example, Cd inhibited the LATS1-MOB1 complex formation, a process independent of Zn (Extended Data Fig. 8a).

Common amino acid ligands of Zn include Cys, His, Asp and Glu[65-67]. Interestingly, one Cys residue, three His residues and a group of Asp and Glu residues were identified in the LATS1-C3 region (Extended Data Fig. 7n). Actually, we mapped the Zn-binding sites on the LATS1-C3 region but found the LATS1 Zn-binding mutant had no kinase activity, indicating an important role of the Zn-binding sites in maintaining LATS structure and/or activity.

Because Zn deficiency can alter many cellular events[68, 69], we mostly performed pulldown and *in vitro* kinase assays to study its direct effect on LATS. Given a significant increase of cellular Zn upon heavy metal load, the Zn binding-mediated LATS inhibition provides at least one potential mechanism for transducing the overdosed heavy metal signal to LATS for MTF1 activation. The association between transition metals and proteins plays an important

role in many growth-related signaling pathways and cellular events[70-78]. Discovery of such Zn-mediated metal-protein interaction in Hippo pathway regulation not only challenges the current dogma that the Hippo pathway is mainly controlled by protein-protein interaction and protein modification, but also connects the Hippo pathway with various Zn-related signaling events.

Methods

Antibodies and chemicals

For Western blotting, anti-α-tubulin (T6199-200UL, 1:5000 dilution), anti-β-actin (A2228, 1:3000 dilution) and anti-Flag (M2) (F3165-5MG, 1:5000 dilution) antibodies were purchased from Sigma-Aldrich. Anti-Myc (sc-40, 1:500 dilution) and anti-p300 (sc-585, 1:500 dilution) antibodies were obtained from Santa Cruz Biotechnology. Anti-hemagglutinin (HA) antibody (901503, 1:3000 dilution) was obtained from BioLegend. Anti-pan TEAD (13295S, 1:1000 dilution), anti-phospho-YAP (Ser127) (4911S, 1:1000 dilution), anti-YAP/TAZ (8418S, 1:2000 dilution), anti-phospho-LATS1 (Ser909) (9157S, 1:1000 dilution), anti-phospho-LATS1 (Thr1079) (8654S, 1:1000 dilution), anti-LATS1 (3477S, 1:1000 dilution), anti-phospho-MST (Thr180/Thr183) (3681S, 1:1000 dilution), anti-MST1 (3682S, 1:1000 dilution), anti-phospho-MOB1 (Thr35) (8699S, 1:1000 dilution), anti-MOB1 (3863S, 1:2000 dilution), anti-NF2 (12896S, 1:2000 dilution), anti-KIBRA (8774S, 1:1000 dilution), anti-SP1 (9389S, 1:1000 dilution), anti-CBP (7389S, 1:1000 dilution) and anti-C/EBPα (8178T, 1:1000 dilution) antibodies were purchased from Cell Signaling Technology. Anti-MTF1 antibody (NBP1-86380, 1:2000 dilution) was obtained from Novus Biologicals. ATP-γ-S kinase substrate (ab138911), p-Nitrobenzyl mesylate (ab138910) and anti-Thiophosphate ester antibody (ab92670, 1:1000 dilution) were obtained from Abcam. Anti-MAP4K4/HGK antibody (A301-502A-M, 1:2000 dilution) was obtained from Bethyl Laboratories. Anti-phospho-MAP4K2 (Ser170) antibody (AB-PK646, 1:1000 dilution) was purchased from Kinexus. Anti-phospho-MTF1 (Ser152) antibody (1:500 dilution) was raised against keyhole limpet hemocyanin (KLH)-conjugated phospho-peptide CGCPRTY(phospho-S)TAGNLRT, and affinity purified through SulfoLink peptide coupling gel (Thermo Fisher Scientific). The MBP and GST antisera were raised against their full-length proteins, and their polyclonal antibodies (1:5000 dilution) were affinity-purified using an AminoLink Plus Immobilization and Purification Kit (Thermo Fisher Scientific). The YAP and AMOTL2 antibodies were generated as described previously[79].

For immunofluorescent staining, anti-YAP antibody (sc-101199, 1:200 dilution) was purchased from Santa Cruz Biotechnology. Anti-MTF1 antibody (NBP1-86380, 1:200 dilution) was obtained from Novus Biologicals. Anti-Flag (M2) antibody (F3165-5MG, 1:5000 dilution) was purchased from Sigma-Aldrich.

For immunohistochemical staining, anti-MT1A antibody (NBP1-97493, 1:20 dilution) was purchased from Novus Biologicals. Anti-cleaved caspase-3 (9579S, 1:15 dilution) and anti-YAP (14074S, 1:20 dilution) antibodies were purchased from Cell Signaling Technology. Anti-MTF1 antibody (ab236401, 1:20 dilution) was obtained from Abcam. Anti-phospho-MTF1 (Ser152) antibody (1:20 dilution) was raised against keyhole limpet hemocyanin

(KLH)-conjugated phospho-peptide CGCPRTY(phospho-S)TAGNLRT, and affinity purified through SulfoLink peptide coupling gel (Thermo Fisher Scientific).

For chemicals, KCl (P5405), CaCl2 (C7902), MgCl2 (M8266), CdCl2 (655198), MnCl2 (M3634), ZnCl2 (Z0152), Zn(NO3)2 (228737) and ZnSO4 (Z0251) were purchased from Sigma-Aldrich. NaCl (S271-3) was obtained from Fisher Scientific. CuSO4 (7758-98-7) was obtained from Acros Organics. AgNO3 (11414) and FeCl3 (12357) were purchased from Alfa Aesar. Verteporfin (SML0534), TPEN (P4413), ammonium tetrathiomolybdate (TTM) (323446) and carboplatin (C2538) were obtained from Sigma-Aldrich. XMU-MP-1 (6482) was obtained from Tocris. Cisplatin (AG-CR1-3590) was purchased from Adipogen.

Constructs and viruses

Plasmids encoding the indicated genes were obtained from the Human ORFeome V5.1 library or purchased from DNASU Plasmid Repository and Dharmacon. All constructs were generated via polymerase chain reaction (PCR) and subcloned into a pDONOR201 vector as entry clones using Gateway Technology (Thermo Fisher Scientific). Gateway-compatible destination vectors with the indicated SFB tag, Myc tag, HA tag, GST tag and MBP tag were used to express various fusion proteins. PCR-mediated mutagenesis was used to generate all the indicated site mutations. MTF1 luciferase reporter (MREd)6-Luc construct was kindly provided by Dr. Carl Séguin (UniversitéLaval, Québec). The *Drosophila mtf1* construct (clone number: IP15679) was obtained from the *Drosophila* Genomics Resource Center (DGRC) and corrected by PCR to make its coding sequence consistent with NM_140054.3.

All lentiviral supernatants were generated by transient transfection of HEK293T cells with the helper plasmids pSPAX2 and pMD2G (kindly provided by Dr. Zhou Songyang, Baylor College of Medicine) and harvested 48 hours later. Supernatants were passed through a 0.45-μm filter and used to infect cells with the addition of 8 μg/mL hexadimethrine bromide (Polybrene) (Sigma-Aldrich). To express inducible lenti-SFB-tagged proteins close to endogenous level, the stable cells were cultured in medium containing ~50 ng/mL doxycycline (Sigma-Aldrich).

YAP shRNA was purchased from Addgene (#27368). pGIPZ-TAZ shRNA was obtained from MD Anderson Cancer Center shRNA and ORFeome Core Facility with targeting sequence 5′-CAGACATGAGATCCATCACTA-3′.

Cell culture and transfection

HEK293T (a female cell line, ATCC: CRL-3216), Hep3B (a male cell line, ATCC: HB-8064), MCF10A (a female cell line, ATCC: CRL-10317) and HeLa (a female cell line, ATCC: CCL-2) cell lines were purchased from ATCC and kindly provided by Dr. Junjie Chen (MD Anderson Cancer Center). HEK293A (a female cell line, Thermo Fisher Scientific: R70507) cells were kindly provided by Dr. Jae-Il Park (MD Anderson Cancer Center). MCF10 DCIS cells (a female cell line) were kindly provided by Dr. Jing Yang (University of California, San Diego). HEK293T, Hep3B, HeLa and HEK293A cells were maintained in Dulbecco’s modified essential medium (DMEM) supplemented with 10% fetal bovine serum at 37°C in 5% CO_2 (v/v). MCF10A and MCF10 DCIS cells

were maintained in DMEM/F12 medium supplemented with 5% horse serum, 200 ng/mL epidermal growth factor, 500 ng/mL hydrocortisone, 100 ng/mL cholera toxin and 10 μg/mL insulin at 37 °C in 5% CO_2 (v/v). All the culture media contain 1% penicillin and streptomycin.

Plasmid transfection was performed using a polyethylenimine reagent and lipofectamine 3000 (Thermo Fisher Scientific).

Gene inactivation by CRISPR/Cas9 system

The indicated LATS1/2 double knockout (DKO), MOB1A/B DKO, NF2 KO HEK293A cells were generated as described previously[52]. Using the same single-guide RNA (sgRNA) sets[52], we generated the LATS1/2 DKO and MOB1A/B DKO MCF10 DCIS cells. The MST1/2 DKO HEK293A cells were kindly provided by Dr. Kun-Liang Guan (University of California, San Diego).

To generate the MTF1 knockout cells, five sgRNAs were designed by CHOPCHOP website (https://chopchop.rc.fas.harvard.edu), cloned into lentiGuide-Puro vector (Addgene plasmid #52963), and transfected into wild-type and the LATS1/2 DKO HEK293A cells with lentiCas9-Blast construct (Addgene plasmid #52962). Cells were selected with puromycin (2 μg/ml) for two days and subcloned to form single colonies. Knockout cell clones were screened by Western blot to verify the loss of MTF1 expression and their genomic editing was further confirmed by sequencing. The MTF1 sgRNA sequence information is as follows:

MTF1_sgRNA1: 5′-CCTTCAATATTTCTTGGCAT-3′;

MTF1_sgRNA2: 5′-CTCAGGTTTGTGGATAAAAA-3′;

MTF1_sgRNA3: 5′-AACCTGAGCATTTTATCATC-3′;

MTF1_sgRNA4: 5′-GCACATTCGAACTCATACAG-3′;

MTF1_sgRNA5: 5′-AGGGGAAAAGCCATTTCGGT-3′.

Cell viability assay

Same number of cells were seeded in 12-well plates and subjected to the indicated heavy metal treatment. At the endpoint, cells were fixed with 4% paraformaldehyde for 10 min and stained with 0.1% crystal violet. Cells were then washed for 3 times and de-stained with acetic acid. The absorbance of the crystal violet solution was measured at OD 595nm using Gen5 software in a Bio-Tek plate reader and normalized to vehicle-treated cells.

RNA extraction, reverse transcription and real-time PCR

RNA samples were extracted with TRIzol reagent (Invitrogen). Reverse transcription assay was performed with the Script Reverse Transcription Supermix Kit (Bio-Rad) according to the manufacturer's instructions. Real-time PCR was performed using Power SYBR Green PCR master mix (Applied Biosystems) and data were collect by StepOnePlus Real-Time PCR System Software v2.3. For quantification of gene expression, the $2^{-\Delta\Delta Ct}$ method was

used. *GAPDH* expression was used for normalization. The sequence information of q-PCR primers used for gene expression analysis is listed in the Supplementary Table 2.

Immunofluorescent staining

Immunofluorescent staining was performed as described previously[80]. Briefly, cells cultured on coverslips were fixed with 4% paraformaldehyde for 10 minutes at room temperature and then extracted with 0.5% Triton X-100 solution for 5 minutes. After blocking with Tris-buffered saline with Tween 20 containing 1% bovine serum albumin, the cells were incubated with the indicated primary antibodies for 1 hour at room temperature. After that, cells were washed and incubated with fluorescein isothiocyanate- or rhodamine-conjugated secondary antibodies for 1 hour. To visualize nuclear DNA, cells were counterstained with 100 ng/mL 4′,6-diamidino-2-phenylindole (DAPI) for 2 minutes. The cover slips were mounted onto glass slides with an anti-fade solution and visualized under a Nikon Ti2-E inverted microscope. NIS-Elements BR 5.11.01 software was used to collect the data.

RNA sequencing

Total RNAs from wild-type and the LATS1/2 DKO HEK293A cells were extracted by TRIzol reagent (Invitrogen) and used for library preparation. Sequencing was performed using Illumina HiSeq 4000 in the Genomics High-Throughput Facility (GHTF) at the University of California, Irvine. Sequencing reads were aligned to the human reference genome (GRCh38/hg38, Ensembl) using STAR[81]. Differential expression analysis was performed using DEseq2[82] with the cutoffs over 2-fold change and FDR less than 5%. The RNA sequencing dataset is available in Gene Expression Omnibus (GEO) with the accession number GSE163156.

Luciferase reporter assay

For luciferase reporter assay, the indicated HEK239A and HEK293T cells were seeded in 12-well plates the day before transfection. MTF1 luciferase reporter (MREd)6-Luc, PRL-SV40 and indicated plasmids were co-transfected. Twenty-four hours later, cells were lysed and luciferase activity was assayed by Dual-Luciferase Reporter Assay System kit (Promega) following the manufacturer's instructions. The luminescences were measured by a Bio-Tek plate reader with Gen5 software. The measured luciferase activity was normalized to the *Renilla* activity.

Chromatin immunoprecipitation (ChIP) assay

The ChIP assay was modified based on a previous study[83]. Briefly, cells reconstituted with SFB-tagged MTF1 were treated with CdCl2 and ZnCl2 for two hours, cross-linked with 1% formaldehyde for 10 min, and quenched with 0.125 M glycine. After that, cells were lysed in RIPA buffer and sonicated to obtain sheared chromatin. The chromatin lysates were incubated with S protein beads at 4°C overnight. The ChIP DNA was reverse cross-linked, recovered, and quantitated by q-PCR. The primer sequence information is listed in Supplementary Table 2.

Liquid chromatography tandem mass spectrometry (LC MS/MS)

Peptide digests were analyzed by LC MS/MS utilizing an UltiMate 3000 UHPLC (Thermo Fisher Scientific) coupled on-line to an Orbitrap Fusion Lumos mass spectrometer (Thermo Fisher Scientific) as previously described[84]. Protein identification and phosphorylation characterization were done with database searching using the developmental version of Protein prospector. All MS/MS spectra for phosphorylated peptides were further inspected manually.

Recombinant protein production

The GST-fused proteins expressed in *Escherichia coli* were purified by Glutathione Sepharose 4B beads (GE Healthcare) according to the manufacturer's protocol and eluted by glutathione buffer (20 mM L-gluthathione; 150 mM Tris-HCl, pH 8.8). The MBP-fused proteins expressed in *Escherichia coli* were purified by amylose resin (New England Biolabs) according to the manufacturer's protocol and eluted by maltose buffer (10 mM maltose; 20 mM Tris-HCl, pH 7.5; 200 mM NaCl; 1 mM EDTA; 10 mM β-mercaptoethanol).

In vitro kinase assay

Endogenous LATS1, MST1 and MAP4K4 kinases were immunoprecipitated using the indicated antibody and Protein A/G agarose beads (Santa Cruz Biotechnology). SFB-tagged MAP4K2, MAP4K4 and MAP4K6 kinases were purified using S protein beads (Millipore). The isolated kinases were washed 3 times in washing buffer (40 mM HEPES, 250 mM NaCl), once in kinase buffer (30 mM HEPES, 50 mM potassium acetate, 5 mM MgCl2), and subjected to the kinase assay in the presence of cold ATP (500 μM) and 2 μg bacterially-purified GST-YAP, GST-MOB1, MBP-MTF1-R2, or MBP-LATS1-C3 (a region containing LATS1 hydrophobic motif)[52]. The reaction mixture was incubated at 30 °C for 30 min, terminated with 2x SDS loading buffer and subjected to SDS–PAGE. Phosphorylation of YAP, MOB1, MTF1-R2 and LATS1-C3 were determined by anti-phospho-YAP (Ser127), anti-phospho-MOB1 (Thr35), anti-phospho-MTF1 (Ser152), and anti-phospho-LATS1 (Thr1079) antibodies, respectively.

As for ATP-γ-S-based kinase assay, SFB-LATS1 or its kinase dead mutant (K734R) were expressed in HEK293T cells for 48 hours, purified using S protein beads, washed 3 times in washing buffer (40 mM HEPES, 250 mM NaCl), and subjected to kinase assay in the presence of 500 μM ATP-γ-S and 2 μg bacterially-purified MBP-MTF1-truncation proteins. The reaction mixture was incubated at 30 °C for 30 min, supplemented with 2.5 mM p-Nitrobenzyl mesylate (PNBM) at room temperature for 1h, terminated with 2x SDS loading buffer, and subjected to SDS–PAGE. Protein phosphorylation was detected by an anti-Thiophosphate-ester antibody.

Mouse Cd intoxication study

The mouse Cd-intoxication experiments were approved by the Institutional Animal Care and Use Committee (IACUC) and Environmental Health and Safety (EH&S) of University of California, Irvine, and performed under veterinary supervision. The approved IACUC protocol number is AUP-19-113. Briefly, 60 five-week-old female C57BL/6 mice were

purchased from the Jackson Laboratory, and randomly assigned into two groups with one group (15 mice) intraperitoneally injected with H2O control and the other group (45 mice) intraperitoneally injected with CdCl2 (5 mg/kg). One hour later, the CdCl2-intoxicated group of mice were randomly assigned into three sub-groups with 15 mice each, and subjected to the indicated single or combined treatment with vehicle, XMU-MP-1 (3 mg/kg) and Verteporfin (100 mg/kg). Three hours post treatment, three mice from each group were randomly selected and euthanized for tissue analysis. The rest mice were used for survival analysis for another 96 hours. Mice were maintained in the University Laboratory Animal Resources (ULAR) Facility of University of California, Irvine under 12-hour light/12-hour dark cycle (on at 6:30 am/off at 6:30 pm) with temperature of 72 °F ± 2 and 30-70% humidity. The log-rank (i.e. Mantel-Cox) test was performed to analyze the survival differences between groups.

Immunohistochemical analysis

For mouse tissue staining, samples were collected and fixed in 10% formalin. After processing for paraffin embedding, sectioned samples were deparaffinized and rehydrated for hematoxylin and eosin (H&E) staining or immunohistochemical staining. As for immunohistochemical analysis, the antigens were retrieved by applying Unmask Solution (Vector Laboratories) in a steamer for 40 min. To block endogenous peroxidase activity, the sections were treated with 3% hydrogen peroxide for 30 min. After 1 hour of pre-incubation in 10% goat serum to prevent non-specific staining, the samples were incubated with an antibody at 4 °C overnight. The sections were incubated with SignalStain Boost detection reagent at room temperature for 30 min. Color was developed with SignalStain 3,3’-diaminobenzidine chromogen-diluted solution (all reagents were obtained from Cell Signaling Technology). Sections were counterstained with Mayer hematoxylin.

Metal binding assay

Metal beads were generated using Profinity™ IMAC resins (Bio-Rad) according to the manufacturer’s protocol. Briefly, IMAC resins were washed with ultra-pure H2O for 5 times and incubated with 0.2 M indicated metal solution at 4 °C for 2 hours. The metal-charged beads were washed 5 times with ultra-pure H2O, twice with acidic buffer (0.05 M sodium acetate, 0.5 M NaCl, pH 4.0), and stored in binding buffer (0.05 M sodium phosphate, 0.5 M NaCl, pH 8.0) at 4 °C. As for the metal binding assay, cells were lysed in NTN buffer (100 mM NaCl; 20 mM Tris-Cl, pH 8.0; 0.5% Nonidet P-40) supplemented with protease/phosphatase inhibitors and incubated with the indicated metal beads at 4 °C overnight.

Circular dichroism (CD) measurement

CD spectroscopy in the UV region (190 nm~260 nm) was utilized to analyze protein secondary structure. Briefly, 0.2 μg/μL MBP-LATS-C3 or MBP protein was dialyzed and prepared in the CD buffer (137 mM NaF, 2.7 mM KCl, 8 mM Na2HPO4, 2 mM NaH2PO4, pH 7.4) containing ZnCl2 or CaCl2 at the indicated concentrations in a 1-mm cuvette (NSG Precision Cells, Inc., Farmingdale, NY). The CD spectra in 190 nm~260 nm spectral region (50 nm/min and 2 nm spectral resolution) and at 25 °C were collected using a Jasco J-810 spectropolarimeter with Spectra Manager Ver.2 software (JASCO, Easton, MD).

Molecular dynamics simulations

All simulations were performed using the PMEMD program implemented in AMBER18 molecular dynamics suite (https://ambermd.org/). Initial parameterization of the ZAP1-ZAF1 (PDB: 1ZW8)[46] and Zn-bound conformations were conducted with the LEaP module in AMBER18, using the protein force field *ff*14SB[85] and zinc AMBER force field (ZAFF)[86]. The protein was capped with ACE and NHE groups at *N*- and *C*- termini, respectively. To generate the mutant complexes, the Ser 591 from 1ZW8 was mutated into aspartic acid (Asp) using LEaP. Correspondingly, the phosphorylated protein was generated by changing the sidechain of Ser 591 into the phosphorylated state in LEaP. All systems were solvated in a TIP3P truncated octahedron water box and neutralized with either Na^+ or Cl^- counter ions and with additional NaCl added up to 0.1 M. These systems were minimized first followed by a heating process to 320 K for 20 ns and then cooling down to 300 K for 10 ns with a time step of 1 fs in the canonical (NVT) ensemble. They were then equilibrated for 60 ns at 300 K in the isothermal-isobaric (NPT) ensemble. The final production runs were performed in the NVT ensemble with a time step of 2 fs at 300K for 1000 ns. Five independent trajectories with identical starting structures and random initial velocities were generated for the wild-type, mutant, and phosphorylated complexes to enhance sufficient sampling. For all the simulations, the last 500-800 ns trajectory was used for the subsequent analysis to ensure converged calculations. The root-mean-square deviation (RMSD) values were calculated using CPPTRAJ[87]. Snapshots closest to the average structures was used as the representation of the MD-generated conformations. The structure distance measure (SDM)[88] and the Q-score values[89] were also calculated for structure comparison between the wild-type and mutant systems using the UCSF Chimera program.

Fly copper intoxication assay

Heterozygous *mats Drosophila* mutant (stock number 18115) and homozygous *mtf1 Drosophila* mutant (stock number 9241) were obtained from the Bloomington *Drosophila* Stock Center at Indiana University. Adult fly viability was assayed by placing 10 individual adult *Drosophila* (~7-day old) in normal food supplemented with 5 mM CuSO4 and determining the number of survivors daily. Three biological replicates were scored in parallel.

Statistics and reproducibility

Each experiment was repeated twice or more with similar results, unless otherwise noted. There were no samples or animals excluded for the analyses in this study. There was no statistical method used to predetermine sample size. As for the mouse experiments, we assigned the animals randomly to different groups. A laboratory technician was blinded to the group allocation and tissue collection during the animal experiments as well as the data analyses. The two-tailed Student's *t*-test was used to analyze the differences between two sample groups. If each paired sample group compare showed the same *p* value, these sample groups were labeled with only one *p* value. The two-way ANOVA test was used to examine the significance when comparing more than two sample groups. Animal survival data were

analyzed by log-rank (i.e. Mantel-Cox) test. s.d. was used for error estimation. A p value < 0.05 was considered statistically significant.

Extended Data

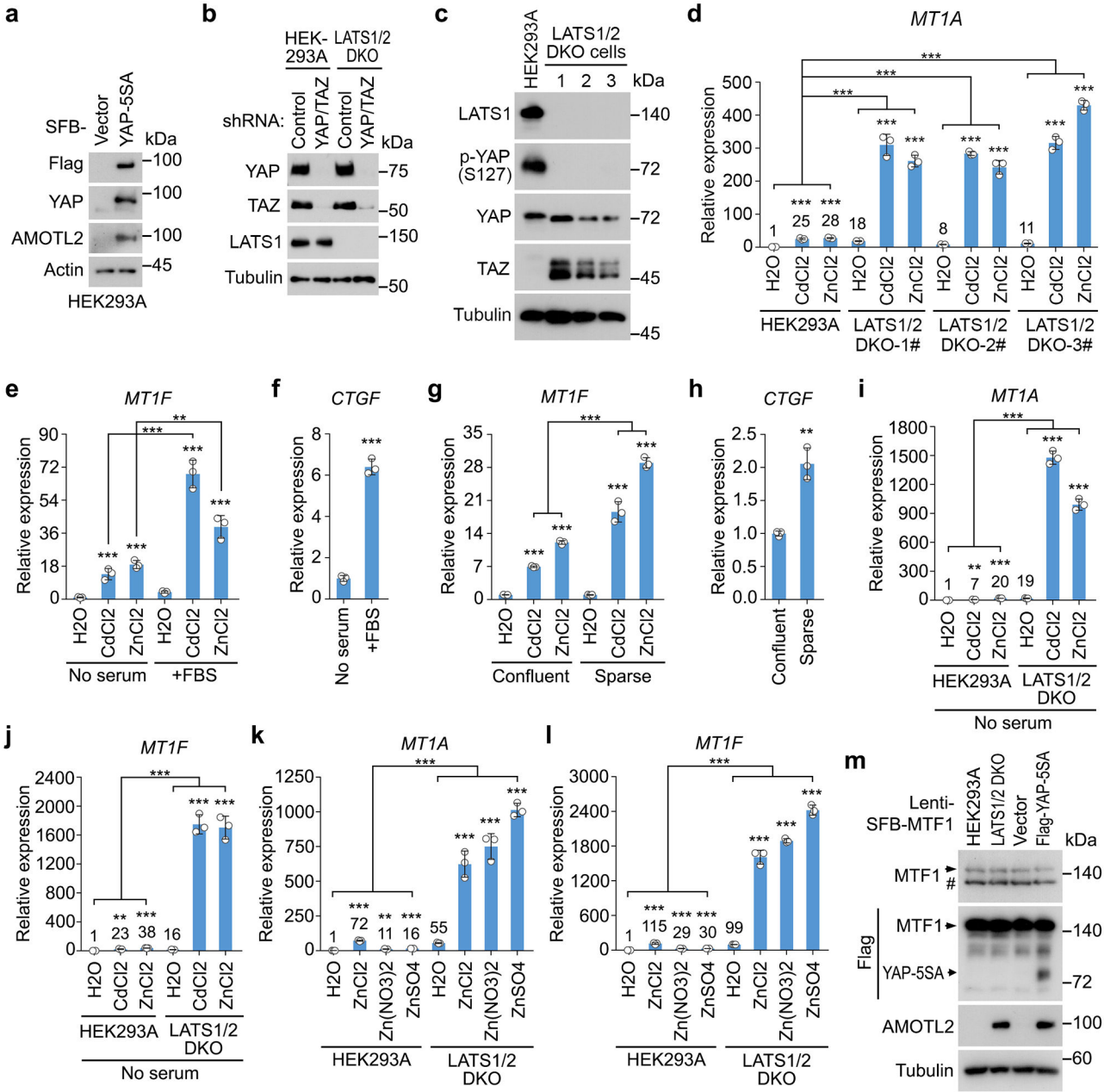

Extended Data Fig. 1. Inhibition of the Hippo pathway activates heavy metal response.

(**a**) Validation of the YAP-5SA overexpressed HEK239A cells. Western blot was performed using the indicated antibodies.

(**b**) Validation of the YAP/TAZ shRNAs-transduced LATS1/2 DKO HEK293A cells. Western blot was performed using the indicated antibodies.

(**c-d**) Western blot was performed using the indicated antibodies (**c**). *MT1A* gene transcription was examined in the indicated cells treated with CdCl2 (50 μM) and ZnCl2 (250 μM) for 4 hours by q-PCR (mean ± s.d., n=3 biological replicates) (**d**). *** $p < 0.001$ (two-tailed Student's *t*-test). Relative expression fold change numbers are shown.
(**e-f**) Transcription of *MT1F* (**e**) and *CTGF* (**f**) was examined in the HEK293A cells cultured under serum starvation and serum stimulation by q-PCR (mean ± s.d., n=3 biological replicates). ** $p < 0.01$, *** $p < 0.001$ (two-tailed Student's *t*-test).
(**g-h**) Transcription of *MT1F* (**g**) and *CTGF* (**h**) was examined in the HEK293A cells cultured under high density and low density by q-PCR (mean ± s.d., n=3 biological replicates). ** $p < 0.01$, *** $p < 0.001$ (two-tailed Student's *t*-test).
(**i-j**) Serum-starved wild-type and the LATS1/2 DKO HEK293A cells were treated with CdCl2 (50 μM) and ZnCl2 (250 μM) for 4 hours. Transcription of *MT1A* (**i**) and *MT1F* (**j**) was examined by q-PCR (mean ± s.d., n=3 biological replicates). ** $p < 0.01$, *** $p < 0.001$ (two-tailed Student's *t*-test). Relative expression fold change numbers are shown.
(**k-l**) Wild-type and the LATS1/2 DKO HEK293A cells were treated with 250 μM Zn with the indicated anions for 4 hours. The transcription of *MT1A* (**i**) and *MT1F* (**j**) was examined by q-PCR (mean ± s.d., n=3 biological replicates). ** $p < 0.01$, *** $p < 0.001$ (two-tailed Student's *t*-test).
(**m**) Validation of the indicated HEK293A cells stably expressing SFB-MTF1. Western blot was performed using the indicated antibodies.
Data shown represent 2 independent experiments in **a-c**, **m**.

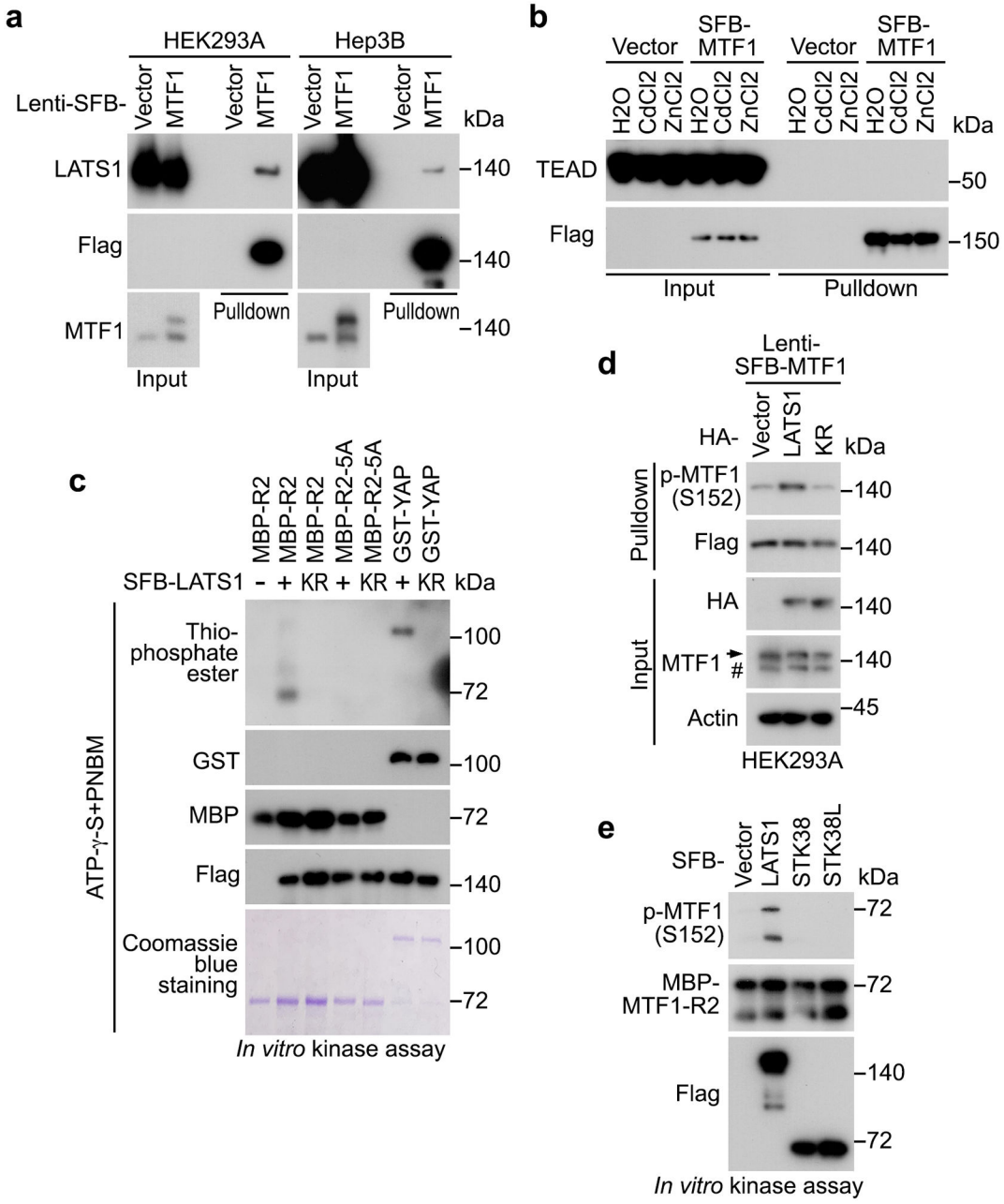

Extended Data Fig. 2. LATS1 binds and phosphorylates MTF1.

(**a**) HEK293A and Hep3B cells stably expressing SFB-tagged MTF1 were subjected to pulldown assay using S protein beads. Western blot was performed using the indicated antibodies.

(**b**) HEK293A cells were transfected with the construct encoding SFB-tagged MTF1, treated with CdCl2 (50 μM) and ZnCl2 (250 μM) for 1 hour, and subjected to pulldown assay using S protein beads. Western blot was performed using the indicated antibodies.

(**c**) SFB-tagged LATS1 and its kinase dead (K734R) mutant were expressed in HEK293T cells, purified using S protein beads, and subjected to the ATP-γ-S-based *in vitro* kinase assay. Bacterially purified MBP-MTF1-R2, MBP-R2-5A mutant (S152A/T153A/T241A/

S301A/T302A) and GST-YAP proteins were used as substrates. Western blot was performed using the indicated antibodies.

(**d**) HEK293A cells stably expressing SFB-tagged MTF1 were transfected with the constructs encoding HA-tagged LATS1 and its kinase dead (K734R) mutant, and subjected to pulldown assay using S protein beads. Western blot was performed using the indicated antibodies. Arrow indicates the exogenously expressed SFB-MTF1. Pound sign indicates endogenous MTF1.

(**e**) SFB-tagged LATS1, STK38 and STK38L were expressed in HEK293T cells, purified using S protein beads, and subjected to *in vitro* kinase assay. Bacterially purified MBP-tagged MTF1-R2 protein was used as substrate. Western blot was performed using the indicated antibodies.

Data shown represent 2 independent experiments in **a**-**e**.

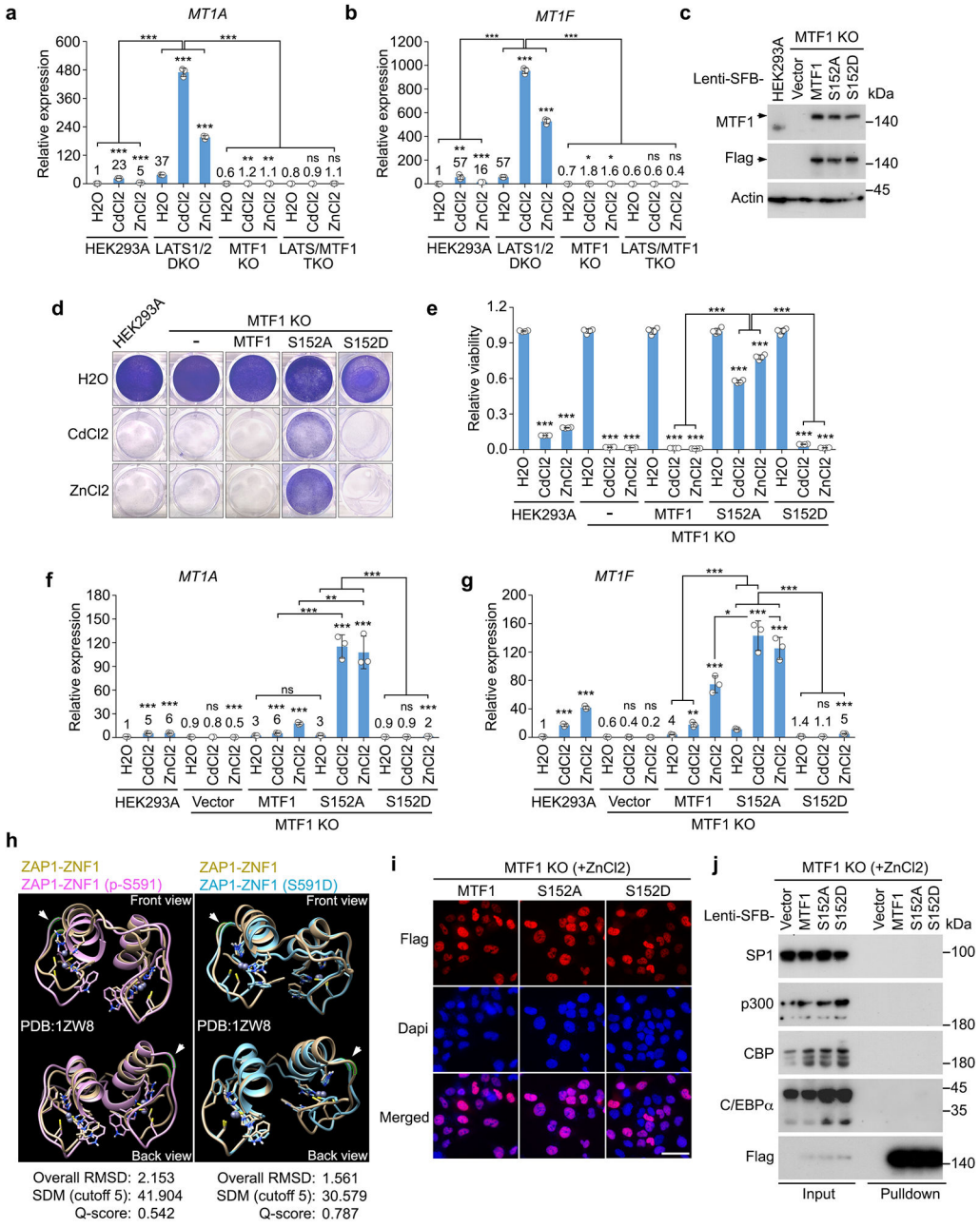

Extended Data Fig. 3. MTF1 S152 phosphorylation inhibits heavy metal response.

(**a-b**) The indicated HEK293A cells were treated with CdCl2 (50 μM) and ZnCl2 (250 μM) for 4 hours. The transcription of *MT1A* (**a**) and *MT1F* (**b**) was examined by q-PCR (mean ± s.d., n=3 biological replicates). * $p < 0.05$, ** $p < 0.01$, *** $p < 0.001$ (two-tailed Student's *t*-test). ns, no significance. Relative expression fold change numbers are shown.

(**c**) Validation of the MTF1 KO HEK293A cells reconstituted with the indicated SFB-tagged MTF1 and its mutants. Western blot was performed using the indicated antibodies. Arrow indicates the exogenously expressed SFB-tagged MTF1 and its mutants.

(**d-e**) The MTF1KO HEK293A cells were reconstituted with the indicated SFB-tagged MTF1 and its mutants, treated with CdCl2 (50 μM) and ZnCl2 (250 μM) for 12 hours,

visualized by crystal violet staining (**d**), and quantified for relative viability (mean ± s.d., n=4 biological replicates) (**e**). *** $p < 0.001$ (two-tailed Student's *t*-test).

(**f-g**) The transcription of *MT1A* (**f**) and *MT1F* (**g**) was examined in wild-type and the MTF1 KO HEK293A cells reconstituted with the indicated SFB-tagged MTF1 and its mutants by q-PCR (mean ± s.d., n=3 biological replicates). Cells were treated with CdCl2 (50 μM) and ZnCl2 (250 μM) for 4 hours. * $p < 0.05$, ** $p < 0.01$, *** $p < 0.001$ (two-tailed Student's *t*-test). ns, no significance.

(**h**) The structure comparison of the ZAP1-ZNF1 in khaki with the phosphorylated ZAP1-ZNF1 (p-S591) in pink (left) and with ZAP1-ZNF1 S591D mutant in blue (right). The overall RMSD values of wild-type ZAP1-ZNF1 with its phosphorylated form (p-S591) and S591D mutant are shown. Arrows indicate the S591 site.

(**i**) The MTF1 KO HEK293A cells were reconstituted with the indicated SFB-MTF1 and its mutants, and treated with ZnCl2 (250 μM) for 1 hour. Immunofluorescent staining was performed. Scale bar, 40 μm. Data shown represent 3 independent experiments.

(**j**) The MTF1 KO HEK293A cells were reconstituted with the indicated SFB-MTF1 and its mutants, treated with ZnCl2 (250 μM) for 1 hour, and subjected to pulldown assay using S protein beads. Western blot was performed using the indicated antibodies.

Data shown represent 2 independent experiments in **c, j**.

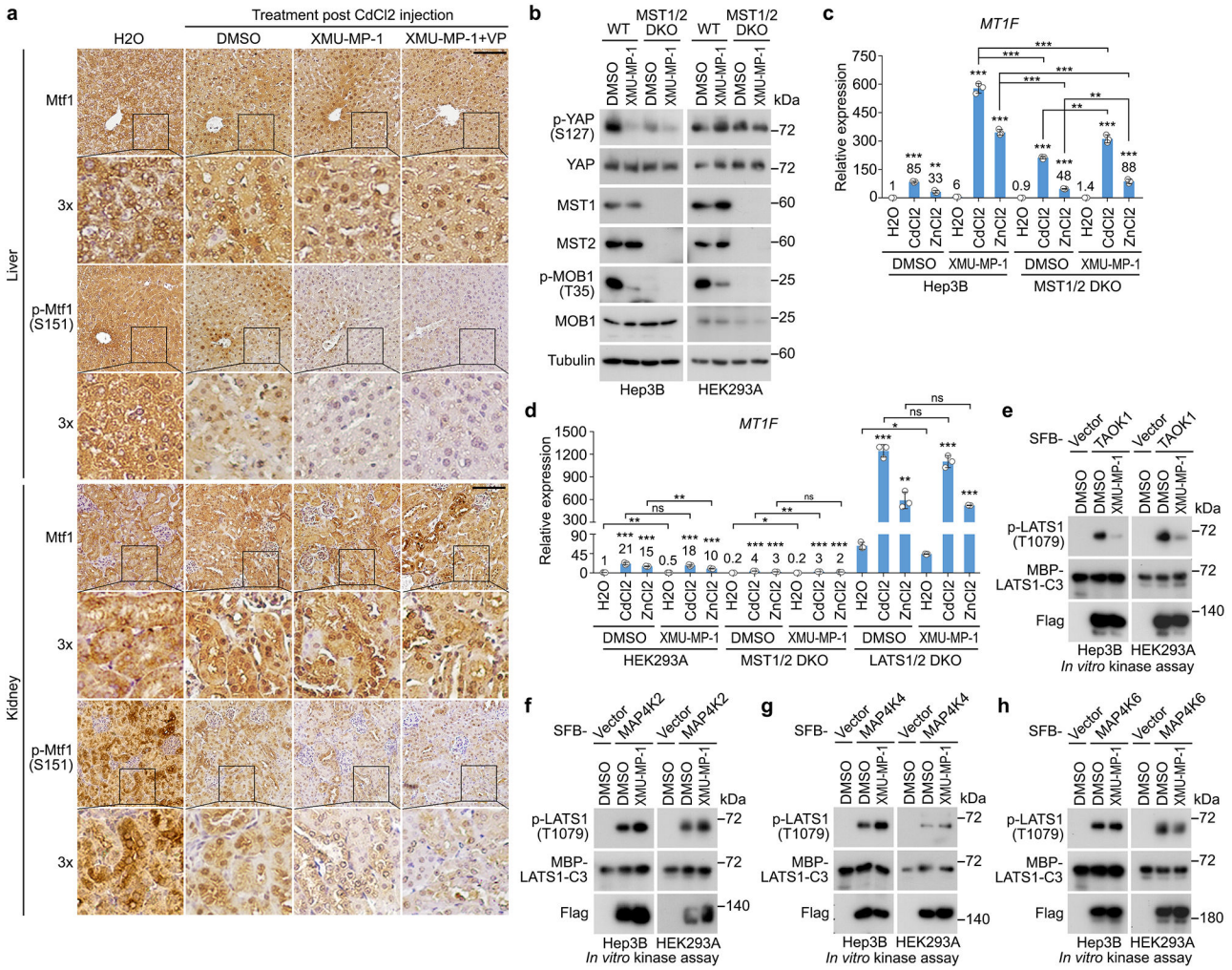

Extended Data Fig. 4. Characterization of XMU-MP-1 in regulating the Hippo pathway and heavy metal response.

(**a**) Immunohistochemical analyses of Mtf1 and its S151 phosphorylation were performed in the liver and kidney tissues of the mice treated with DMSO, XMU-MP-1 alone or combined with VP post CdCl2 intoxication. The indicated regions in the box are shown 3 times enlarged. Scale bar, 150 μM. Data shown represent 3 independent experiments.

(**b**) Wild-type and the MST1/2 DKO Hep3B and HEK293A cells were treated with DMSO and XMU-MP-1 (10 μM) for 4 hours, and subjected to Western blot analysis using the indicated antibodies.

(**c-d**) The indicated Hep3B cells (**c**) and HEK293A cells (**d**) were pre-incubated with XMU-MP-1 (10 μM) for 2 hours, and treated with CdCl2 (50 μM) and ZnCl2 (250 μM) for 4 hours. The transcription of *MT1F* was examined by q-PCR (mean ± s.d., n=3 biological replicates). * $p < 0.05$, ** $p < 0.01$, *** $p < 0.001$ (two-tailed Student's *t*-test). ns, no significance.

(**e-h**) Hep3B and HEK293A cells stably expressing SFB-tagged TAOK1 (**e**), MAP4K2 (**f**), MAP4K4 (**g**) and MAP4K6 (**h**) were serum starved for 24 hours, and treated with XMU-MP-1 (10 μM) for 4 hours. The indicated SFB-tagged kinases were purified using S protein

beads and subjected to *in vitro* kinase assay using the bacterially purified MBP-tagged LATS1-C3 protein as substrate. Western blot was performed using the indicated antibodies Data shown represent 2 independent experiments in **b, e-h**.

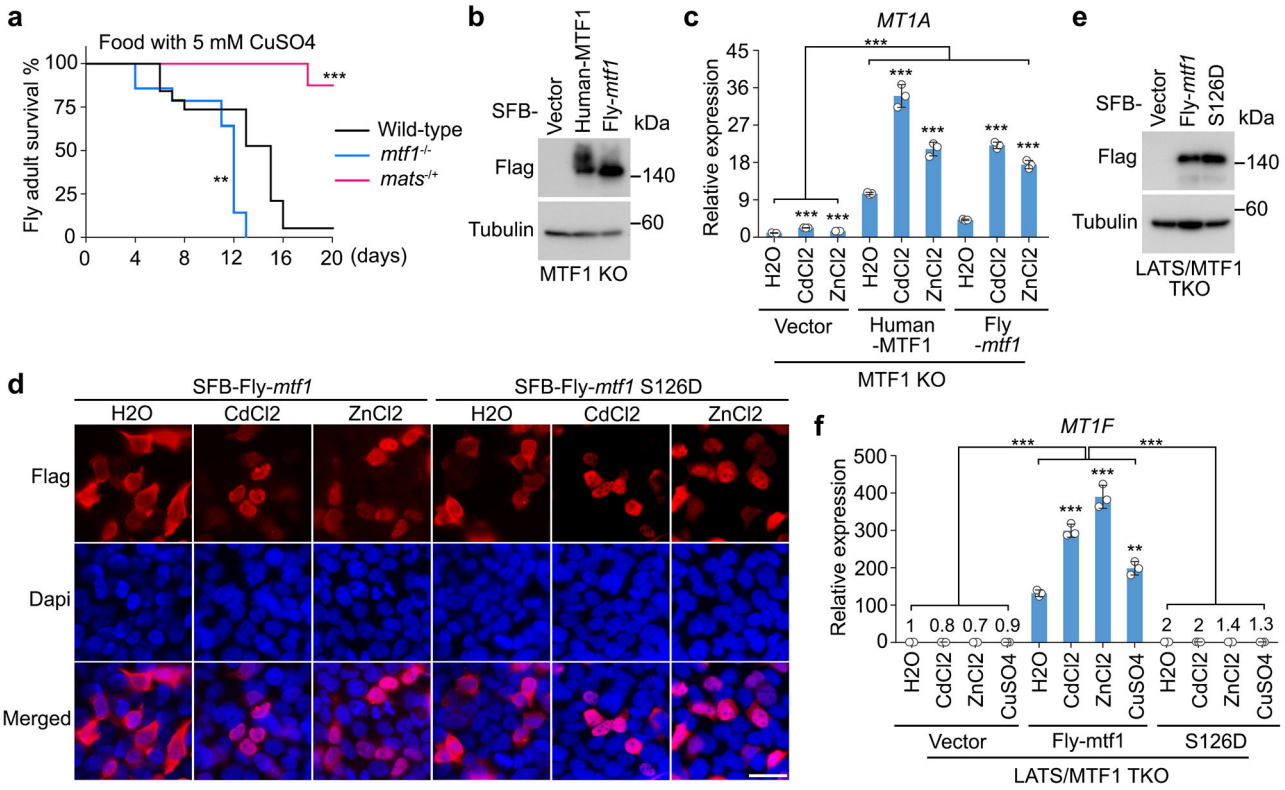

Extended Data Fig. 5. The Hippo pathway-mediated regulation of MTF1 and heavy metal response is conserved in *Drosophila*.

(**a**) Heterozygous *mats Drosophila* mutant and homozygous *mtf1 Drosophila* mutant were used for adult viability assay. Adult viability was assayed by feeding adult *Drosophila* (~7-day old) with normal food supplemented with 5 mM CuSO4 and determining the number of survivors daily. **, $p < 0.01$; ***, $p < 0.001$ (Log-rank test). n = 19 for wild-type *Drosophila*, n = 14 for $mtf^{-/-}$ *Drosophila*, n = 24 for $mats^{-/-}$ *Drosophila*.

(**b**) The MTF1 KO HEK293A cells were transfected with the constructs encoding the SFB-tagged human MTF1 and fly-*mtf1*. Western blot was performed using the indicated antibodies.

(**c**) The MTF1 KO HEK293A cells were transfected with the constructs encoding the SFB-tagged human MTF1 and fly-*mtf1*, and treated with CdCl2 (50 μM) and ZnCl2 (250 μM) for 4 hours. *MT1A* gene transcription was examined by q-PCR (mean ± s.d., n=3 biological replicates). *** $p < 0.001$ (two-tailed Student's *t*-test).

(**d**) HEK293A cells were transfected with the constructs encoding the SFB-tagged fly-*mtf1* and its S126D mutant, treated with CdCl2 (50 μM) and ZnCl2 (250 μM) for 1 hour, and subjected to immunofluorescent staining. Scale bar, 40 μm.

(**e**) The LATS/MTF1 TKO HEK293A cells were transduced with the constructs encoding the SFB-tagged fly-*mtf1* and its S126D mutant. Western blot was performed using the indicated antibodies.

(**f**) The LATS/MTF1 TKO HEK293A cells stably expressing the SFB-tagged fly-*mtf1* and its S126D mutant were treated with CdCl2 (50 μM), ZnCl2 (250 μM) and CuSO4 (250 μM) for 4 hours. *MT1F* gene transcription was examined by q-PCR (mean ± s.d., n=3 biological replicates). ** $p < 0.01$, *** $p < 0.001$ (two-tailed Student's *t*-test).
Data shown represent 2 independent experiments in **b**, **d**, **e**.

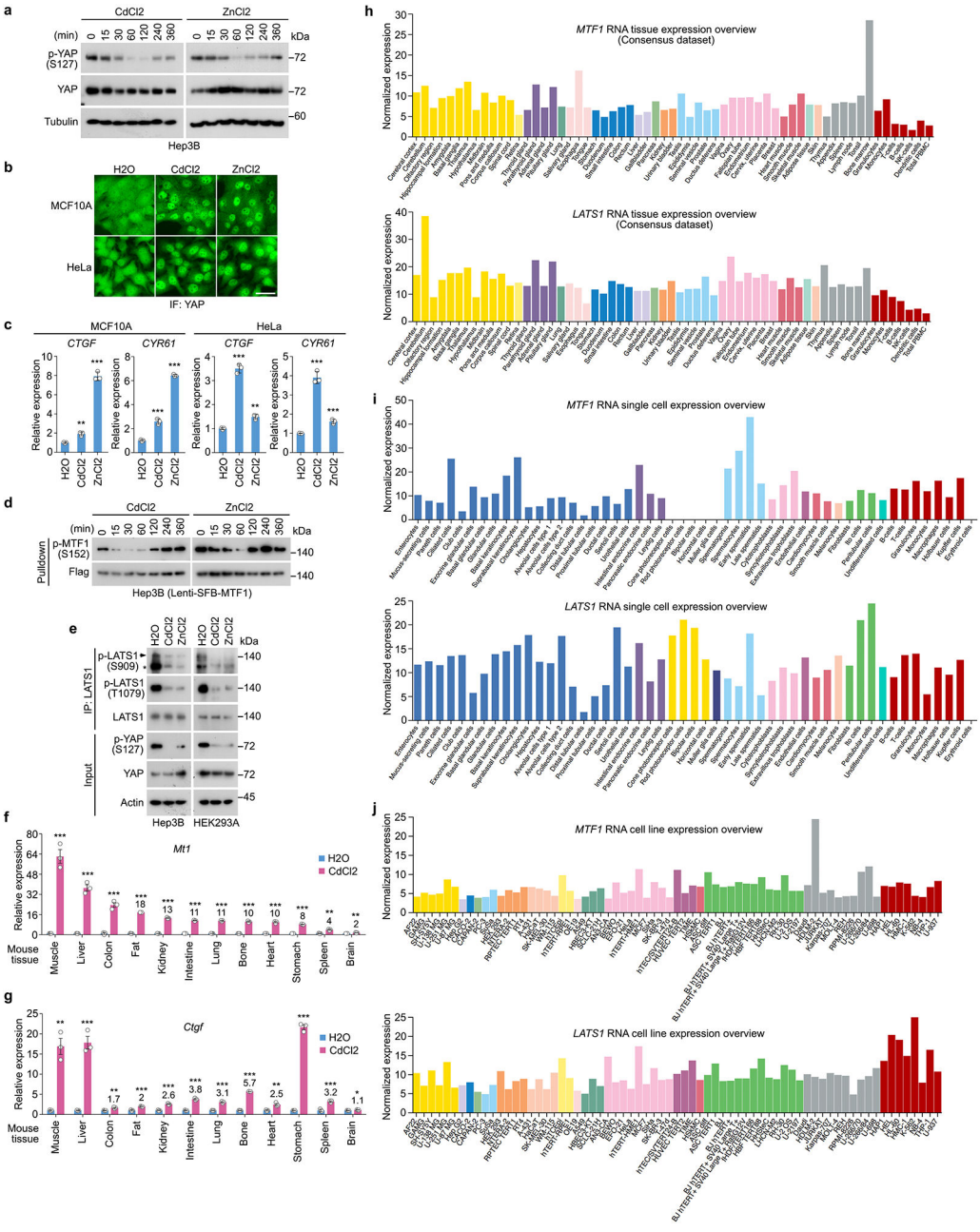

Extended Data Fig. 6. Heavy metals inhibit the Hippo pathway in different cells and tissues.
(**a**) Hep3B cells were serum starved for 24 hours, and treated with CdCl2 (50 μM) and ZnCl2 (250 μM) for the indicated time points. Western blot was performed using the indicated antibodies.

(**b**) MCF10A and HeLa cells were serum starved for 24 hours, treated with CdCl2 (50 μM) and ZnCl2 (250 μM) for 1 hour, and subjected to immunofluorescent staining. Scale bar, 40 μm.

(**c**) MCF10A and HeLa cells were serum starved for 24 hours, and treated with CdCl2 (50 μM) and ZnCl2 (250 μM) for 4 hours. The transcription of YAP downstream genes *CTGF* and *CYR61* was examined by q-PCR (mean ± s.d., n = 3 biological replicates). ** $p < 0.01$, *** $p < 0.001$ (two-tailed Student's *t*-test).

(**d**) Hep3B cells stably expressing SFB-tagged MTF1 were serum starved for 24 hours, treated with CdCl2 (50 μM) and ZnCl2 (250 μM) for the indicated time points, and subjected to pulldown assay using S protein beads. Western blot was performed using the indicated antibodies.

(**e**) Hep3B and HEK293A cells were serum starved for 24 hours, treated with CdCl2 (50 μM) and ZnCl2 (250 μM) for 1 hour, and subjected to immunoprecipitation using LATS1 antibody. Western blot was performed using the indicated antibodies. Arrow indicates the correct p-LATS1 S909 signal. Asterisk indicates the non-specific signal.

(**f**) The transcription of heavy metal response gene *Mt1* was examined by q-PCR (mean ± s.d., n = 3 biological replicates). ** $p < 0.01$, *** $p < 0.001$ (two-tailed Student's *t*-test). Relative expression fold change numbers are shown.

(**g**) The transcription of Yap downstream gene *Ctgf* was examined by q-PCR (mean ± s.d., n = 3 biological replicates). * $p < 0.05$, ** $p < 0.01$, *** $p < 0.001$ (two-tailed Student's *t*-test). Relative expression fold change numbers are shown.

(**h-j**) The Human Protein Atlas (https://www.proteinatlas.org/) was used to examine the expression of *MTF1* and *LATS1* in different human tissues (**h**), human cells (**i**) and commonly used human cell lines (**j**).

Data shown represent 2 independent experiments in **a**, **b**, **d**, **e**.

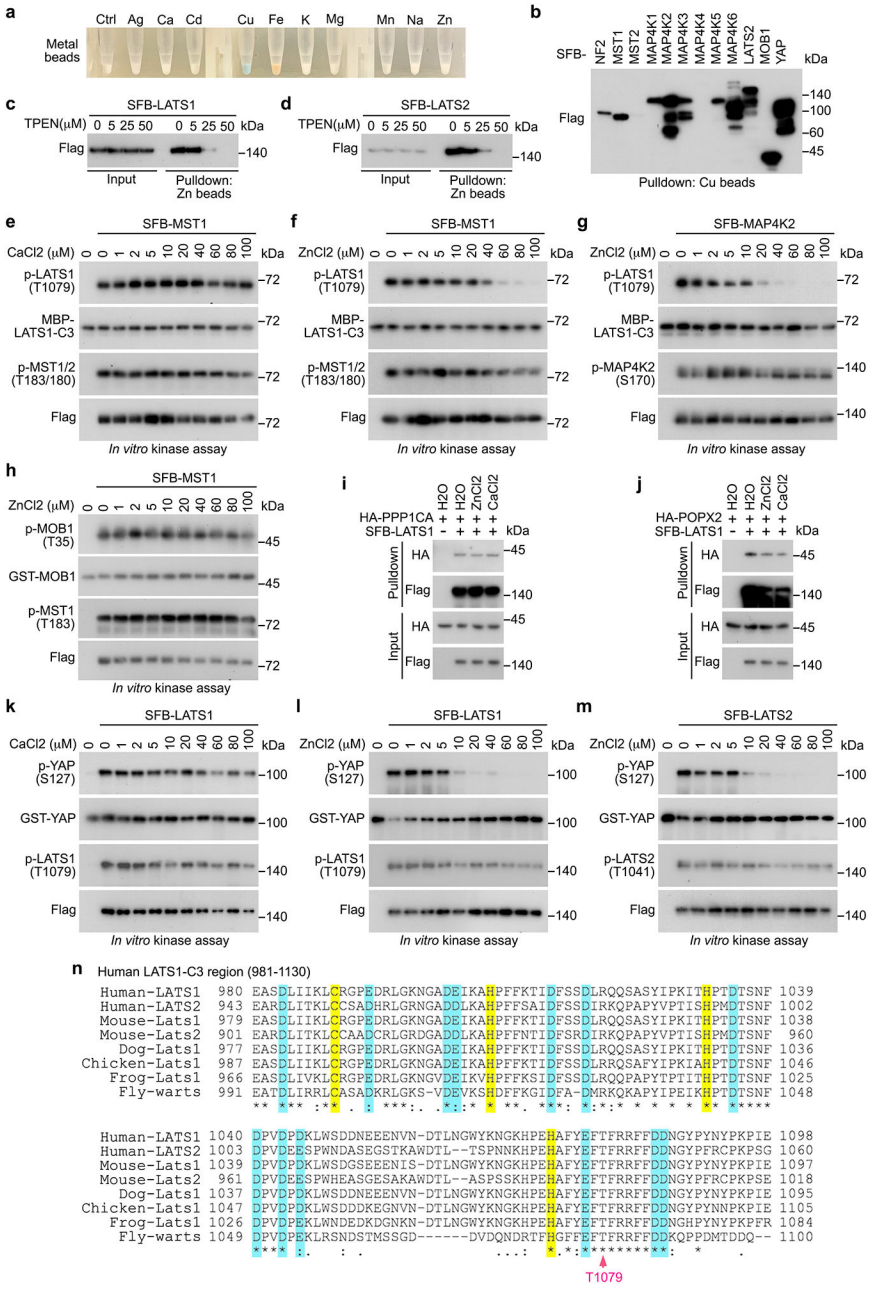

Extended Data Fig. 7. Zn binds and inhibits LATS.

(**a**) Illustration of the metal beads.

(**b**) HEK293T cells were transfected with the constructs encoding the indicated Hippo pathway components and subjected to pulldown assay using Cu beads. The input blot is shared with the one in Fig. 8c.

(**c-d**) HEK293T cells were transfected with the constructs encoding SFB-tagged LATS1 (**c**) and LATS2 (**d**), and subjected to pulldown assay using Zn beads in the presence of TPEN at the indicated concentrations.

(**e-f**) SFB-tagged MST1 was expressed in HEK293T cells, purified using S protein beads, and subjected to *in vitro* kinase assay in the presence of CaCl2 (**e**) and ZnCl2 (**f**) at the indicated concentrations. MBP-tagged LATS1-C3 protein was used as substrate.
(**g**) SFB-tagged MAP4K2 was expressed in HEK293T cells, purified using S protein beads, and subjected to *in vitro* kinase assay in the presence of ZnCl2 at the indicated concentrations. MBP-tagged LATS1-C3 protein was used as substrate.
(**h**) SFB-tagged MST1 was expressed in HEK293T cells, purified using S protein beads, and subjected to *in vitro* kinase assay in the presence of ZnCl2 at the indicated concentrations. GST-tagged MOB1 protein was used as substrate.
(**i-j**) HEK293A cells were transfected with the constructs encoding the SFB-tagged LATS1 with HA-tagged PPP1CA (**i**) and POPX2 (**j**), treated with ZnCl2 (250 μM) and CaCl2 (250 μM) for 1 hour, and subjected to pulldown assay using S protein beads.
(**k-l**) SFB-tagged LATS1 was expressed in HEK293T cells, purified using S protein beads, and subjected to *in vitro* kinase assay in the presence of CaCl2 (**k**) or ZnCl2 (**l**) at the indicated concentrations. GST-tagged YAP protein was used as substrate.
(**m**) SFB-tagged LATS2 was expressed in HEK293T cells, purified using S protein beads, and subjected to *in vitro* kinase assay in the presence of ZnCl2 at the indicated concentrations. GST-tagged YAP protein was used as substrate.
(**n**) The potential Zn-binding Cys, His, Glu and Asp residues in the LATS1-C3 region are shown. The conserved Cys and His residues are highlighted in yellow. The conserved Glu and Asp residues are highlighted in blue. LATS1 T1079 site is indicated by arrow.
Data shown represent 2 independent experiments in **b-m**.

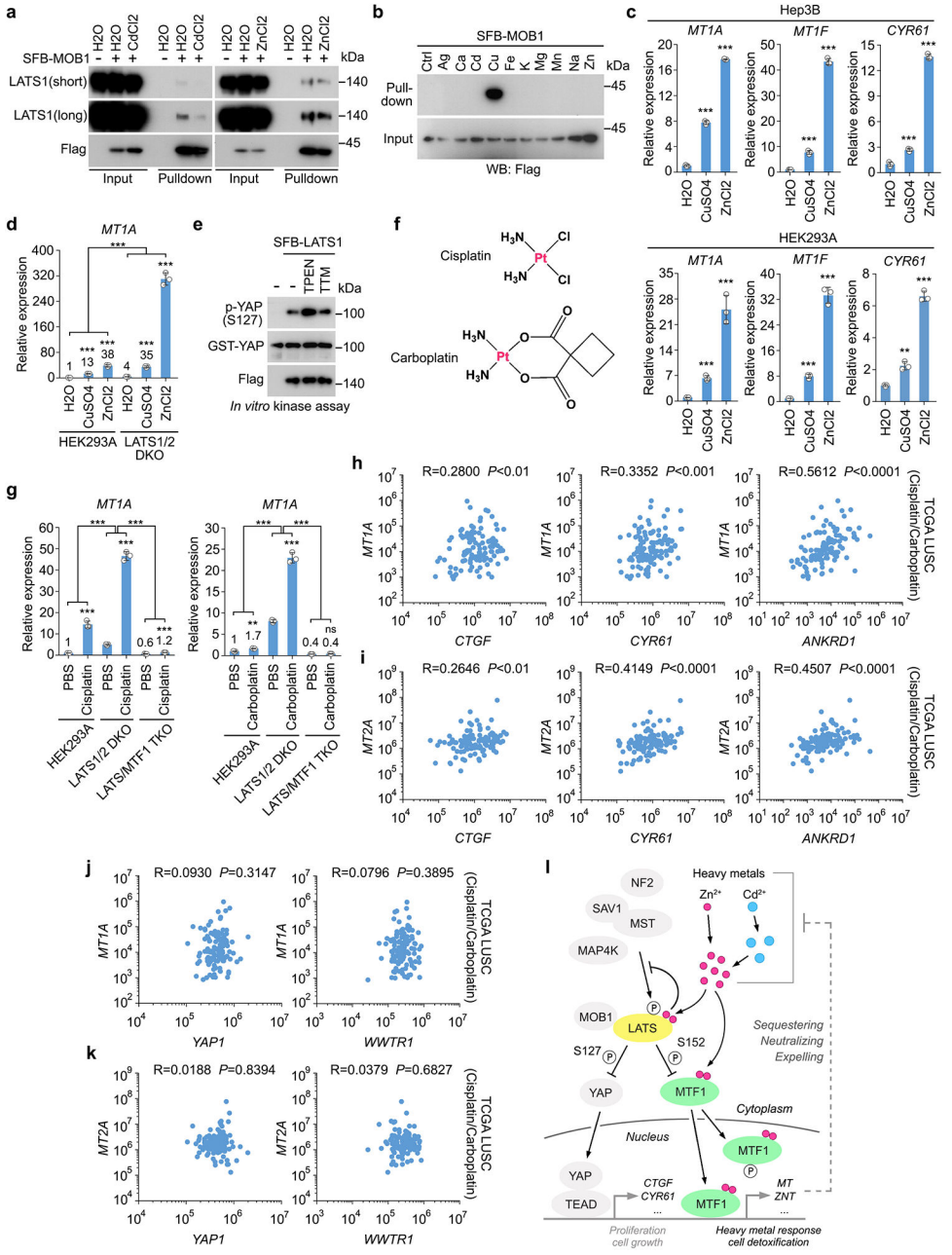

Extended Data Fig. 8. The Hippo pathway mediates cellular response to different heavy metals.

(**a**) HEK293A cells were transfected with the construct encoding SFB-tagged MOB1, treated with CdCl2 (50 μM) and ZnCl2 (250 μM) for 1 hour, and subjected to pulldown assay using S protein beads. Western blot was performed using the indicated antibodies. short, short exposure; long, long exposure.

(**b**) HEK293T cells were transfected with the construct encoding SFB-tagged MOB1 and subjected to pulldown assay using the indicated metal beads.

(**c**) Hep3B and HEK293A cells were serum starved for 24 hours and treated with CuSO4 (250 μM) and ZnCl2 (250 μM) for 4 hours. The transcription of *MT1A*, *MT1F* and *CYR61*

was examined by q-PCR (mean ± s.d., n = 3 biological replicates). ** $p < 0.01$, *** $p < 0.001$ (two-tailed Student's *t*-test).

(**d**) The indicated cells were treated with CuSO4 (250 μM) and ZnCl2 (250μM) for 4 hours. The transcription of *MT1A* was examined by q-PCR (mean ± s.d., n=3 biological replicates). *** $p < 0.001$ (two-tailed Student's *t*-test).

(**e**) SFB-tagged LATS1 was expressed in HEK293T cells, purified using S protein beads, washed thoroughly with high-salt buffer containing 250 mM NaCl, incubated with Zn chelator TPEN (25 μM) or Cu chelator TTM (25 μM), and subjected to *in vitro* kinase assay. GST-YAP protein used as substrate.

(**f**) Illustration of cisplatin and carboplatin compound structures, where platinum is labeled in red.

(**g**) The indicated cells were treated with cisplatin (10 μM) and carboplatin (100 μM) for 6 hours. The transcription of *MT1A* was examined by q-PCR (mean ± s.d., n=3 biological replicates). ** $p < 0.05$, *** $p < 0.001$ (two-tailed Student's *t*-test). ns, no significance. Relative expression fold change numbers are shown.

(**h-k**) The lung squamous cell carcinoma (LUSC) RNAseq datasets with clinic data were downloaded from the Cancer Genome Atlas (TCGA) data portal. The indicated gene expression from a total of 119 patients treated with cisplatin or carboplatin were subjected to Spearman correction analysis. Correlation coefficient *R* value and *p* value were calculated by GraphPad prism software.

(**l**) A proposed model for the Hippo pathway-mediated heavy metal response through MTF1. Data shown represent 2 independent experiments in **a**, **b**, **e**.

Supplementary Material

Refer to Web version on PubMed Central for supplementary material.

Acknowledgments

We thank Drs. Kun-Liang Guan (University of California San Diego), Duojia Pan (The University of Texas Southwestern Medical Center), David Fruman (University of California, Irvine) and Aimee Edinger (University of California, Irvine) for comments on this study. We thank Drs. Justin Wai Chung Leung (University of Arkansas for Medical Sciences), Robert Edwards (University of California, Irvine), Grant MacGregor (University of California, Irvine) and Roger Geertsema (University of California, Irvine) for technical help. This work was supported by NIH grants (R01GM126048, R21ES031642), American Cancer Society Research Scholar grant (RSG-18-009-01-CCG), University of California Cancer Research Coordinating Committee Research Award (CRN-19-585568), and Tower Cancer Research Foundation Cancer Free Generation Career Development Grant to W.W., and also supported in part by NIH grants to R.L. (R35GM130367), K.W.Y.C (R35GM139617) and L.H. (R01GM130144). W.W. is a member of the Chao Family Comprehensive Cancer Center (P30CA062203) at University of California, Irvine.

Data availability

The RNA sequencing dataset is available in Gene Expression Omnibus (GEO) with the accession number GSE163156. The lung squamous cell carcinoma (LUSC) RNAseq datasets were downloaded from the Cancer Genome Atlas (TCGA) data portal (https://portal.gdc.cancer.gov/). The protein structure information (PDB: 1ZW8) is downloaded from protein data bank (https://www.rcsb.org/structure/1zw8). Source data are provided with this paper. All other data supporting the findings of this study are available from the corresponding author on reasonable request.

References

1. Gunther V, Lindert U & Schaffner W The taste of heavy metals: gene regulation by MTF-1. Biochim Biophys Acta 1823, 1416–1425 (2012). [PubMed: 22289350]
2. Sharma B, Singh S & Siddiqi NJ Biomedical implications of heavy metals induced imbalances in redox systems. Biomed Res Int 2014, 640754 (2014). [PubMed: 25184144]
3. Planchart A, Green A, Hoyo C & Mattingly CJ Heavy Metal Exposure and Metabolic Syndrome: Evidence from Human and Model System Studies. Curr Environ Health Rep 5, 110–124 (2018). [PubMed: 29460222]
4. Baltaci AK, Yuce K & Mogulkoc R Zinc Metabolism and Metallothioneins. Biol Trace Elem Res (2017).
5. Coyle P, Philcox JC, Carey LC & Rofe AM Metallothionein: the multipurpose protein. Cell Mol Life Sci 59, 627–647 (2002). [PubMed: 12022471]
6. Nath R, Kambadur R, Gulati S, Paliwal VK & Sharma M Molecular aspects, physiological function, and clinical significance of metallothioneins. Crit Rev Food Sci Nutr 27, 41–85 (1988). [PubMed: 3293923]
7. Hamer DH Metallothionein. Annu Rev Biochem 55, 913–951 (1986). [PubMed: 3527054]
8. Robbins AH et al. Refined crystal structure of Cd, Zn metallothionein at 2.0 A resolution. J Mol Biol 221, 1269–1293 (1991). [PubMed: 1942051]
9. Dong G, Chen H, Qi M, Dou Y & Wang Q Balance between metallothionein and metal response element binding transcription factor 1 is mediated by zinc ions (review). Mol Med Rep 11, 1582–1586 (2015). [PubMed: 25405524]
10. Davis SR & Cousins RJ Metallothionein expression in animals: a physiological perspective on function. J Nutr 130, 1085–1088 (2000). [PubMed: 10801901]
11. Stuart GW, Searle PF & Palmiter RD Identification of multiple metal regulatory elements in mouse metallothionein-I promoter by assaying synthetic sequences. Nature 317, 828–831 (1985). [PubMed: 4058587]
12. Westin G & Schaffner W A zinc-responsive factor interacts with a metal-regulated enhancer element (MRE) of the mouse metallothionein-I gene. EMBO J 7, 3763–3770 (1988). [PubMed: 3208749]
13. Radtke F et al. Cloned transcription factor MTF-1 activates the mouse metallothionein I promoter. EMBO J 12, 1355–1362 (1993). [PubMed: 8467794]
14. Brugnera E et al. Cloning, chromosomal mapping and characterization of the human metal-regulatory transcription factor MTF-1. Nucleic Acids Res 22, 3167–3173 (1994). [PubMed: 8065932]
15. Lindert U, Cramer M, Meuli M, Georgiev O & Schaffner W Metal-responsive transcription factor 1 (MTF-1) activity is regulated by a nonconventional nuclear localization signal and a metal-responsive transactivation domain. Mol Cell Biol 29, 6283–6293 (2009). [PubMed: 19797083]
16. Bittel D, Dalton T, Samson SL, Gedamu L & Andrews GK The DNA binding activity of metal response element-binding transcription factor-1 is activated in vivo and in vitro by zinc, but not by other transition metals. J Biol Chem 273, 7127–7133 (1998). [PubMed: 9507026]
17. Egli D et al. Knockout of 'metal-responsive transcription factor' MTF-1 in Drosophila by homologous recombination reveals its central role in heavy metal homeostasis. EMBO J 22, 100–108 (2003). [PubMed: 12505988]
18. Gunes C et al. Embryonic lethality and liver degeneration in mice lacking the metal-responsive transcriptional activator MTF-1. EMBO J 17, 2846–2854 (1998). [PubMed: 9582278]
19. Wang Y et al. Metal-responsive transcription factor-1 (MTF-1) is essential for embryonic liver development and heavy metal detoxification in the adult liver. FASEB J 18, 1071–1079 (2004). [PubMed: 15226267]
20. Hua H et al. Toxicity of Alzheimer's disease-associated Abeta peptide is ameliorated in a Drosophila model by tight control of zinc and copper availability. Biol Chem 392, 919–926 (2011). [PubMed: 21801085]

21. Saini N, Georgiev O & Schaffner W The parkin mutant phenotype in the fly is largely rescued by metal-responsive transcription factor (MTF-1). Mol Cell Biol 31, 2151–2161 (2011). [PubMed: 21383066]
22. Shi Y et al. The metal-responsive transcription factor-1 protein is elevated in human tumors. Cancer Biol Ther 9, 469–476 (2010). [PubMed: 20087061]
23. Yu FX, Zhao B & Guan KL Hippo Pathway in Organ Size Control, Tissue Homeostasis, and Cancer. Cell 163, 811–828 (2015). [PubMed: 26544935]
24. Halder G & Johnson RL Hippo signaling: growth control and beyond. Development 138, 9–22 (2011). [PubMed: 21138973]
25. Pan D The hippo signaling pathway in development and cancer. Dev Cell 19, 491–505 (2010). [PubMed: 20951342]
26. Yu FX & Guan KL The Hippo pathway: regulators and regulations. Genes Dev 27, 355–371 (2013). [PubMed: 23431053]
27. Piccolo S, Dupont S & Cordenonsi M The biology of YAP/TAZ: hippo signaling and beyond. Physiol Rev 94, 1287–1312 (2014). [PubMed: 25287865]
28. Zanconato F, Cordenonsi M & Piccolo S YAP/TAZ at the Roots of Cancer. Cancer Cell 29, 783–803 (2016). [PubMed: 27300434]
29. Zheng Y et al. Identification of Happyhour/MAP4K as Alternative Hpo/Mst-like Kinases in the Hippo Kinase Cascade. Dev Cell 34, 642–655 (2015). [PubMed: 26364751]
30. Li S, Cho YS, Yue T, Ip YT & Jiang J Overlapping functions of the MAP4K family kinases Hppy and Msn in Hippo signaling. Cell Discov 1, 15038 (2015). [PubMed: 27462435]
31. Meng Z et al. MAP4K family kinases act in parallel to MST1/2 to activate LATS1/2 in the Hippo pathway. Nat Commun 6, 8357 (2015). [PubMed: 26437443]
32. Li Q et al. The conserved misshapen-warts-Yorkie pathway acts in enteroblasts to regulate intestinal stem cells in Drosophila. Dev Cell 31, 291–304 (2014). [PubMed: 25453828]
33. Li Q et al. Ingestion of Food Particles Regulates the Mechanosensing Misshapen-Yorkie Pathway in Drosophila Intestinal Growth. Dev Cell 45, 433–449 e436 (2018). [PubMed: 29754801]
34. Boggiano JC, Vanderzalm PJ & Fehon RG Tao-1 phosphorylates Hippo/MST kinases to regulate the Hippo-Salvador-Warts tumor suppressor pathway. Dev Cell 21, 888–895 (2011). [PubMed: 22075147]
35. Poon CL, Lin JI, Zhang X & Harvey KF The sterile 20-like kinase Tao-1 controls tissue growth by regulating the Salvador-Warts-Hippo pathway. Dev Cell 21, 896–906 (2011). [PubMed: 22075148]
36. Plouffe SW et al. Characterization of Hippo Pathway Components by Gene Inactivation. Mol Cell 64, 993–1008 (2016). [PubMed: 27912098]
37. Hamaratoglu F et al. The tumour-suppressor genes NF2/Merlin and Expanded act through Hippo signalling to regulate cell proliferation and apoptosis. Nat Cell Biol 8, 27–36 (2006). [PubMed: 16341207]
38. Yin F et al. Spatial organization of Hippo signaling at the plasma membrane mediated by the tumor suppressor Merlin/NF2. Cell 154, 1342–1355 (2013). [PubMed: 24012335]
39. Yu FX, Meng Z, Plouffe SW & Guan KL Hippo pathway regulation of gastrointestinal tissues. Annu Rev Physiol 77, 201–227 (2015). [PubMed: 25293527]
40. Wu S, Liu Y, Zheng Y, Dong J & Pan D The TEAD/TEF family protein Scalloped mediates transcriptional output of the Hippo growth-regulatory pathway. Dev Cell 14, 388–398 (2008). [PubMed: 18258486]
41. Goulev Y et al. SCALLOPED interacts with YORKIE, the nuclear effector of the hippo tumor-suppressor pathway in Drosophila. Curr Biol 18, 435–441 (2008). [PubMed: 18313299]
42. Zhang L et al. The TEAD/TEF family of transcription factor Scalloped mediates Hippo signaling in organ size control. Dev Cell 14, 377–387 (2008). [PubMed: 18258485]
43. Yu FX et al. Regulation of the Hippo-YAP pathway by G-protein-coupled receptor signaling. Cell 150, 780–791 (2012). [PubMed: 22863277]
44. Zhao B et al. Inactivation of YAP oncoprotein by the Hippo pathway is involved in cell contact inhibition and tissue growth control. Genes Dev 21, 2747–2761 (2007). [PubMed: 17974916]

45. Hao Y, Chun A, Cheung K, Rashidi B & Yang X Tumor suppressor LATS1 is a negative regulator of oncogene YAP. J Biol Chem 283, 5496–5509 (2008). [PubMed: 18158288]
46. Wang Z et al. Solution structure of a Zap1 zinc-responsive domain provides insights into metalloregulatory transcriptional repression in Saccharomyces cerevisiae. J Mol Biol 357, 1167–1183 (2006). [PubMed: 16483601]
47. Li Y, Kimura T, Huyck RW, Laity JH & Andrews GK Zinc-induced formation of a coactivator complex containing the zinc-sensing transcription factor MTF-1, p300/CBP, and Sp1. Mol Cell Biol 28, 4275–4284 (2008). [PubMed: 18458062]
48. Datta J et al. Metallothionein expression is suppressed in primary human hepatocellular carcinomas and is mediated through inactivation of CCAAT/enhancer binding protein alpha by phosphatidylinositol 3-kinase signaling cascade. Cancer Res 67, 2736–2746 (2007). [PubMed: 17363595]
49. Fan F et al. Pharmacological targeting of kinases MST1 and MST2 augments tissue repair and regeneration. Sci Transl Med 8, 352ra108 (2016).
50. Chen X et al. Copper sensing function of Drosophila metal-responsive transcription factor-1 is mediated by a tetranuclear Cu(I) cluster. Nucleic Acids Res 36, 3128–3138 (2008). [PubMed: 18411209]
51. Selvaraj A et al. Metal-responsive transcription factor (MTF-1) handles both extremes, copper load and copper starvation, by activating different genes. Genes Dev 19, 891–896 (2005). [PubMed: 15833915]
52. Han H et al. Regulation of the Hippo Pathway by Phosphatidic Acid-Mediated Lipid-Protein Interaction. Mol Cell 72, 328–340 e328 (2018). [PubMed: 30293781]
53. Lv XB et al. PARD3 induces TAZ activation and cell growth by promoting LATS1 and PP1 interaction. EMBO Rep 16, 975–985 (2015). [PubMed: 26116754]
54. Rahmat MB, Zhang S & Koh CG POPX2 is a novel LATS phosphatase that regulates the Hippo pathway. Oncotarget 10, 1525–1538 (2019). [PubMed: 30863499]
55. Rottenberg S, Disler C & Perego P The rediscovery of platinum-based cancer therapy. Nat Rev Cancer 21, 37–50 (2021). [PubMed: 33128031]
56. Chen PH et al. Kinome screen of ferroptosis reveals a novel role of ATM in regulating iron metabolism. Cell Death Differ 27, 1008–1022 (2020). [PubMed: 31320750]
57. LaRochelle O, Gagne V, Charron J, Soh JW & Seguin C Phosphorylation is involved in the activation of metal-regulatory transcription factor 1 in response to metal ions. J Biol Chem 276, 41879–41888 (2001). [PubMed: 11551972]
58. Murphy JT et al. Histidine protects against zinc and nickel toxicity in Caenorhabditis elegans. PLoS Genet 7, e1002013 (2011). [PubMed: 21455490]
59. Bafaro E, Liu Y, Xu Y & Dempski RE The emerging role of zinc transporters in cellular homeostasis and cancer. Signal Transduct Target Ther 2 (2017).
60. Yang H & Shu Y Cadmium transporters in the kidney and cadmium-induced nephrotoxicity. Int J Mol Sci 16, 1484–1494 (2015). [PubMed: 25584611]
61. Gupta A & Lutsenko S Human copper transporters: mechanism, role in human diseases and therapeutic potential. Future Med Chem 1, 1125–1142 (2009). [PubMed: 20454597]
62. Garrick MD Human iron transporters. Genes Nutr 6, 45–54 (2011). [PubMed: 21437029]
63. Tsang T, Davis CI & Brady DC Copper biology. Curr Biol 31, R421–R427 (2021). [PubMed: 33974864]
64. Zhang B et al. Activity of metal-responsive transcription factor 1 by toxic heavy metals and H2O2 in vitro is modulated by metallothionein. Mol Cell Biol 23, 8471–8485 (2003). [PubMed: 14612393]
65. Pace NJ & Weerapana E Zinc-binding cysteines: diverse functions and structural motifs. Biomolecules 4, 419–434 (2014). [PubMed: 24970223]
66. Srivastava A & Kumar M Prediction of zinc binding sites in proteins using sequence derived information. J Biomol Struct Dyn 36, 4413–4423 (2018). [PubMed: 29241411]
67. Shu N, Zhou T & Hovmoller S Prediction of zinc-binding sites in proteins from sequence. Bioinformatics 24, 775–782 (2008). [PubMed: 18245129]

68. Beyersmann D & Haase H Functions of zinc in signaling, proliferation and differentiation of mammalian cells. Biometals 14, 331–341 (2001). [PubMed: 11831463]
69. Maret W Zinc in Cellular Regulation: The Nature and Significance of "Zinc Signals". Int J Mol Sci 18 (2017).
70. Brady DC et al. Copper is required for oncogenic BRAF signalling and tumorigenesis. Nature 509, 492–496 (2014). [PubMed: 24717435]
71. Tsang T et al. Copper is an essential regulator of the autophagic kinases ULK1/2 to drive lung adenocarcinoma. Nat Cell Biol 22, 412–424 (2020). [PubMed: 32203415]
72. Turski ML et al. A novel role for copper in Ras/mitogen-activated protein kinase signaling. Mol Cell Biol 32, 1284–1295 (2012). [PubMed: 22290441]
73. Weinman S Calcium-binding proteins: an overview. J Biol Buccale 19, 90–98 (1991). [PubMed: 1864864]
74. Bialasek M et al. Exploiting iron-binding proteins for drug delivery. J Physiol Pharmacol 70 (2019).
75. Karlsson M & Kurz T Attenuation of iron-binding proteins in ARPE-19 cells reduces their resistance to oxidative stress. Acta Ophthalmol 94, 556–564 (2016). [PubMed: 27287874]
76. Tristao GB et al. Predicting copper-, iron-, and zinc-binding proteins in pathogenic species of the Paracoccidioides genus. Front Microbiol 5, 761 (2014). [PubMed: 25620964]
77. Sanchez M et al. Iron regulatory protein-1 and −2: transcriptome-wide definition of binding mRNAs and shaping of the cellular proteome by iron regulatory proteins. Blood 118, e168–179 (2011). [PubMed: 21940823]
78. Piovesan D, Profiti G, Martelli PL & Casadio R The human "magnesome": detecting magnesium binding sites on human proteins. BMC Bioinformatics 13 Suppl 14, S10 (2012).
79. Wang W, Huang J & Chen J Angiomotin-like proteins associate with and negatively regulate YAP1. J Biol Chem 286, 4364–4370 (2011). [PubMed: 21187284]
80. Wang W, Chen L, Ding Y, Jin J & Liao K Centrosome separation driven by actin-microfilaments during mitosis is mediated by centrosome-associated tyrosine-phosphorylated cortactin. J Cell Sci 121, 1334–1343 (2008). [PubMed: 18388321]
81. Dobin A et al. STAR: ultrafast universal RNA-seq aligner. Bioinformatics 29, 15–21 (2013). [PubMed: 23104886]
82. Love MI, Huber W & Anders S Moderated estimation of fold change and dispersion for RNA-seq data with DESeq2. Genome Biol 15, 550 (2014). [PubMed: 25516281]
83. Lee TI, Johnstone SE & Young RA Chromatin immunoprecipitation and microarray-based analysis of protein location. Nat Protoc 1, 729–748 (2006). [PubMed: 17406303]
84. Wang X et al. The proteasome-interacting Ecm29 protein disassembles the 26S proteasome in response to oxidative stress. J Biol Chem 292, 16310–16320 (2017). [PubMed: 28821611]
85. Maier JA et al. ff14SB: Improving the Accuracy of Protein Side Chain and Backbone Parameters from ff99SB. J Chem Theory Comput 11, 3696–3713 (2015). [PubMed: 26574453]
86. Peters MB et al. Structural Survey of Zinc Containing Proteins and the Development of the Zinc AMBER Force Field (ZAFF). J Chem Theory Comput 6, 2935–2947 (2010). [PubMed: 20856692]
87. Roe DR & Cheatham TE 3rd PTRAJ and CPPTRAJ: Software for Processing and Analysis of Molecular Dynamics Trajectory Data. J Chem Theory Comput 9, 3084–3095 (2013). [PubMed: 26583988]
88. Johnson MS, Sutcliffe MJ & Blundell TL Molecular anatomy: phyletic relationships derived from three-dimensional structures of proteins. J Mol Evol 30, 43–59 (1990). [PubMed: 2107323]
89. Krissinel E & Henrick K Secondary-structure matching (SSM), a new tool for fast protein structure alignment in three dimensions. Acta Crystallogr D Biol Crystallogr 60, 2256–2268 (2004). [PubMed: 15572779]

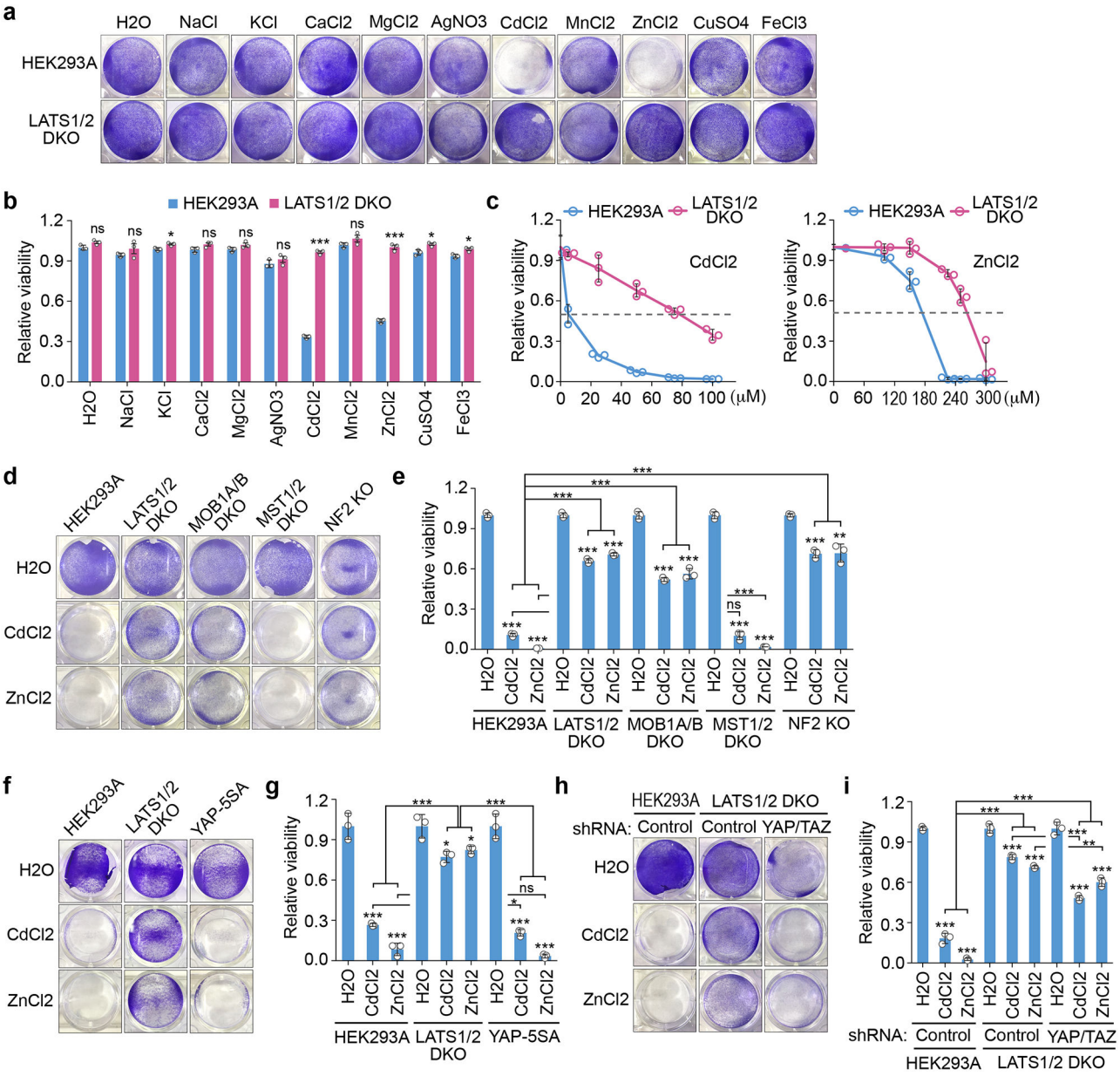

Fig. 1: Hippo signaling deficiency protects cells against heavy metal-induced toxicity.

(**a-b**) Wild-type and the LATS1/2 double knockout (DKO) HEK293A cells were treated with the indicated metals at concentration of 250 μM except CdCl2 (50 μM) and AgNO3 (50 μM) for 12 hours, visualized by crystal violet staining (**a**) and quantified for relative viability (mean ± s.d., n=3 biological replicates) (**b**). * $p < 0.05$, *** $p < 0.001$ (two-tailed Student's *t*-test). ns, no significance.

(**c**) Wild-type and the LATS1/2 DKO HEK293A cells were treated with the indicated concentration of CdCl2 and ZnCl2 for 12 hours, visualized by crystal violet staining, and quantified for relative viability (mean ± s.d., n=3 biological replicates).

(**d-e**) The indicated Hippo pathway component knockout cells were treated with CdCl2 (50 μM) and ZnCl2 (250 μM) for 12 hours, visualized by crystal violet staining (**d**), and

quantified for relative viability (mean ± s.d., n=3 biological replicates) (**e**). ** $p < 0.01$, *** $p < 0.001$ (two-tailed Student's *t*-test). ns, no significance.

(**f-g**) The indicated cells were treated with CdCl2 (50 μM) and ZnCl2 (250 μM) for 12 hours, visualized by crystal violet staining (**f**), and quantified for relative viability (mean ± s.d., n=3 biological replicates) (**g**). * $p < 0.05$, *** $p < 0.001$ (two-tailed Student's *t*-test). ns, no significance.

(**h-i**) The indicated cells were treated with CdCl2 (50 μM) and ZnCl2 (250 μM) for 12 hours, visualized by crystal violet staining (**h**), and quantified for relative viability (mean ± s.d., n=3 biological replicates) (**i**). ** $p < 0.01$, *** $p < 0.001$ (two-tailed Student's *t*-test). ns, no significance.

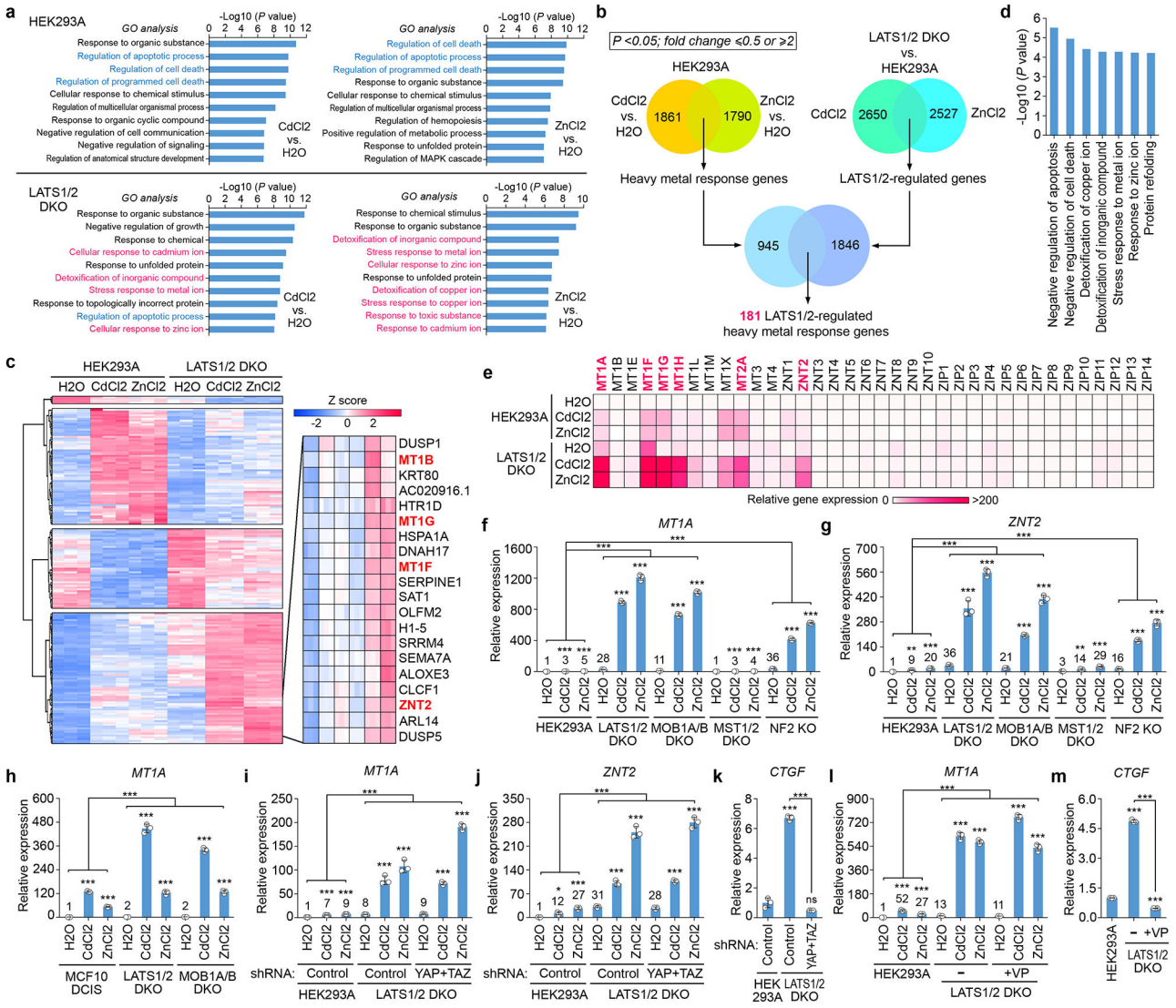

Fig. 2: Hippo signaling deficiency induces heavy metal response gene expression.

(**a**) Genes with their expression at least two folds significantly changed upon Cd/Zn treatment were subjected to GO analysis. *P* values were generated by Gene Ontology Resources (http://geneontology.org/). No statistical test was used. RNAseq was performed in 3 biological replicates and data shown represent an average from these replicates.

(**b**) Comparative RNAseq analysis reveals a total of 181 genes that are regulated by both Cd/Zn and LATS1/2. Gene number for each dataset was shown.

(**c**) Hierarchical clustering analysis of the 181 genes that are regulated by both Cd/Zn and LATS1/2. Among them, metallothioneins (MTs) genes and *ZNT2* were highlighted in red.

(**d**) GO analysis of the *MTs* and *ZNT2*-containing gene set in (**c**).

(**e**) q-PCR screen of the metallothionein (MT), ZNT (SLC30A) and ZIP (SLC39A) family genes in wild-type and the LATS1/2 DKO HEK293A cells under the treatment with H2O, CdCl2 (50 μM) and ZnCl2 (250 μM) for 4 hours. Relative gene expression was shown as the heatmap.

(**f-h**) The transcription of heavy metal response genes *MT1A* (**f**) and *ZNT2* (**g**) was examined in the indicated HEK293A cells by q-PCR (mean ± s.d., n=3 biological replicates). *MT1A* gene expression was examined in the indicated MCF10 DCIS cells by q-PCR (mean ± s.d., n=3 biological replicates) (**h**). Cells were treated with H2O, CdCl2 (50 μM) and ZnCl2 (250 μM) for 4 hours. ** $p < 0.01$, *** $p < 0.001$ (two-tailed Student's *t*-test).

(**i-k**) The transcription of *MT1A* (**i**), *ZNT2* (**j**) and *CTGF* (**k**) was examined in the indicated cells by q-PCR (mean ± s.d., n=3 biological replicates). Cells were treated with H2O, CdCl2 (50 μM) and ZnCl2 (250 μM) for 4 hours. * $p < 0.05$, *** $p < 0.001$ (two-tailed Student's *t*-test). ns, no significance.

(**l-m**) The transcription of *MT1A* (**l**) and *CTGF* (**m**) was examined in the VP-treated LATS1/2 DKO HEK293A cells by q-PCR (mean ± s.d., n=3 biological replicates). The indicated cells were treated with VP (10 mM) for 12 hours and subjected to the treatment with H2O, CdCl2 (50 μM) and ZnCl2 (250 μM) for 4 hours. *** $p < 0.001$ (two-tailed Student's *t*-test).

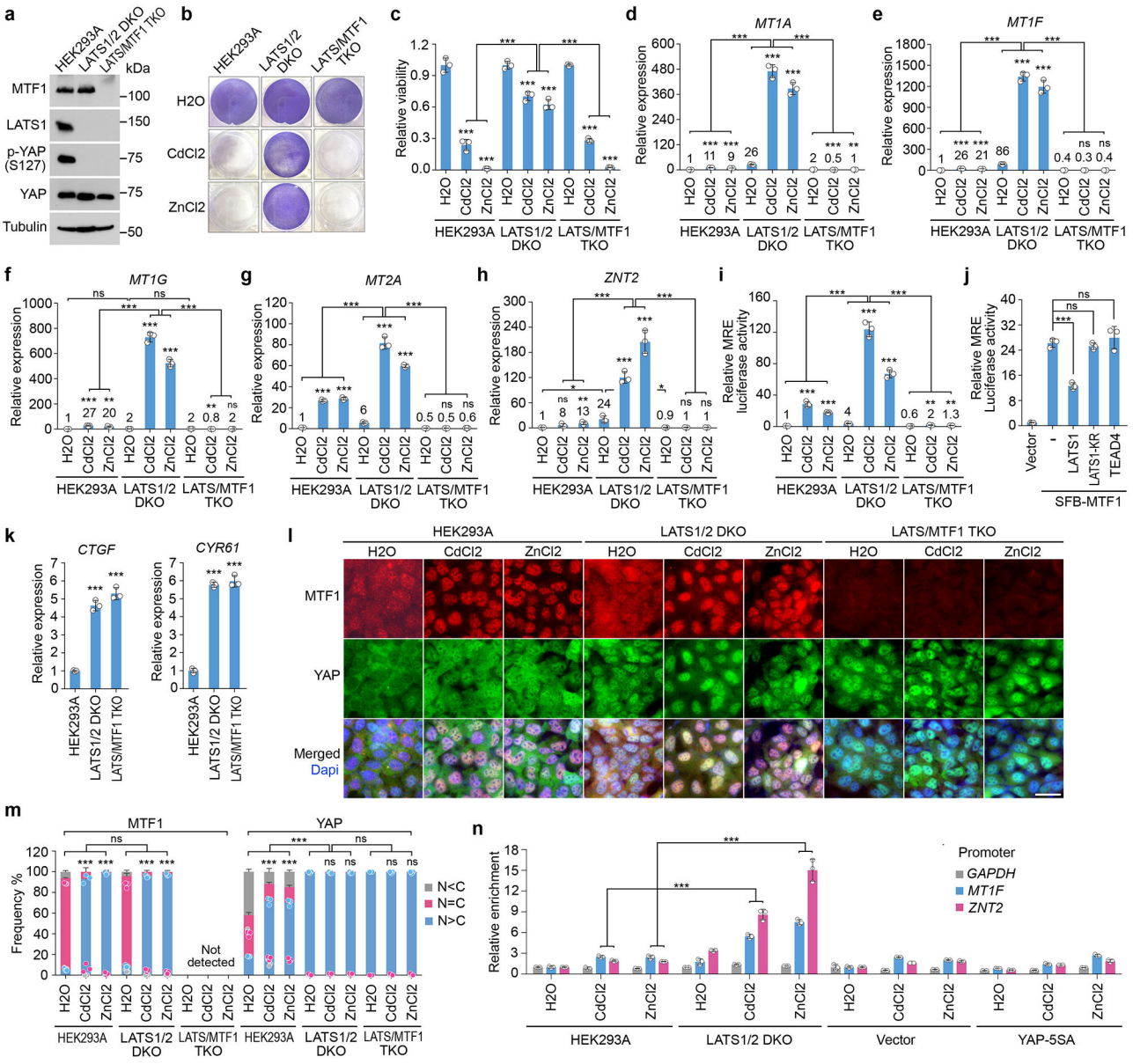

Fig. 3: The Hippo pathway controls heavy metal response by inhibiting MTF1's transcriptional activity.

(**a**) Western blot was performed using the indicated antibodies. Data shown represent 2 independent experiments.

(**b-h**) The indicated cells were treated with CdCl2 (50 μM) and ZnCl2 (250 μM) for 12 hours, visualized by crystal violet staining (**b**), and quantified for relative viability (mean ± s.d., n=3 biological replicates) (**c**). The transcription of *MT1A* (**d**), *MT1F* (**e**), *MT1G* (**f**), *MT2A* (**g**) and *ZNT2* (**h**) was examined by q-PCR (mean ± s.d., n=3 biological replicates). * $p < 0.05$, ** $p < 0.01$, *** $p < 0.001$ (two-tailed Student's *t*-test). ns, no significance.

(**i**) MRE luciferase reporter assay was performed using the indicated cells, where firefly *Renilla* was used as internal control (mean ± s.d., n=3 biological replicates). The indicated

cells were treated with H2O, CdCl2 (50 μM) and ZnCl2 (250 μM) for 4 hours. ** $p < 0.01$, *** $p < 0.001$ (two-tailed Student's *t*-test).

(**j**) MRE luciferase reporter assay was performed by co-transfecting MTF1 construct with that encoding LATS1, LATS1-KR mutant or TEAD4 in HEK293T cells, where firefly *Renilla* was used as internal control (mean ± s.d., n=3 biological replicates). *** $p < 0.001$ (two-tailed Student's *t*-test). ns, no significance.

(**k**) The transcription of *CTGF* and *CYR61* was examined in the indicated cells by q-PCR (mean ± s.d., n=3 biological replicates). *** $p < 0.001$ (two-tailed Student's *t*-test).

(**l-m**) The indicated cells were treated with H2O, CdCl2 (50 μM) and ZnCl2 (250 μM) for 1 hour, and subjected to immunofluorescent staining using the indicated antibody (**l**). Around 60 cells in total were randomly selected and quantified for the MTF1 and YAP subcellular localization (mean ± s.d., n=3 biological replicates) (**m**). Scale bar, 40 μm. The average fluorescence intensity for YAP and MTF1 between nucleus (N) and cytoplasm (C) in each cell was compared. *** $p < 0.001$ (two-way AVONA test). ns, no significance.

(**n**) The indicated cells stably expressing SFB-MTF1 were treated with H2O, CdCl2 (50 μM) and ZnCl2 (250 μM) for 2 hours, and subjected to ChIP assay using S protein beads. The precipitated DNA was quantified by q-PCR (mean ± s.d., n=3 biological replicates). *** $p < 0.001$ (two-tailed Student's *t*-test).

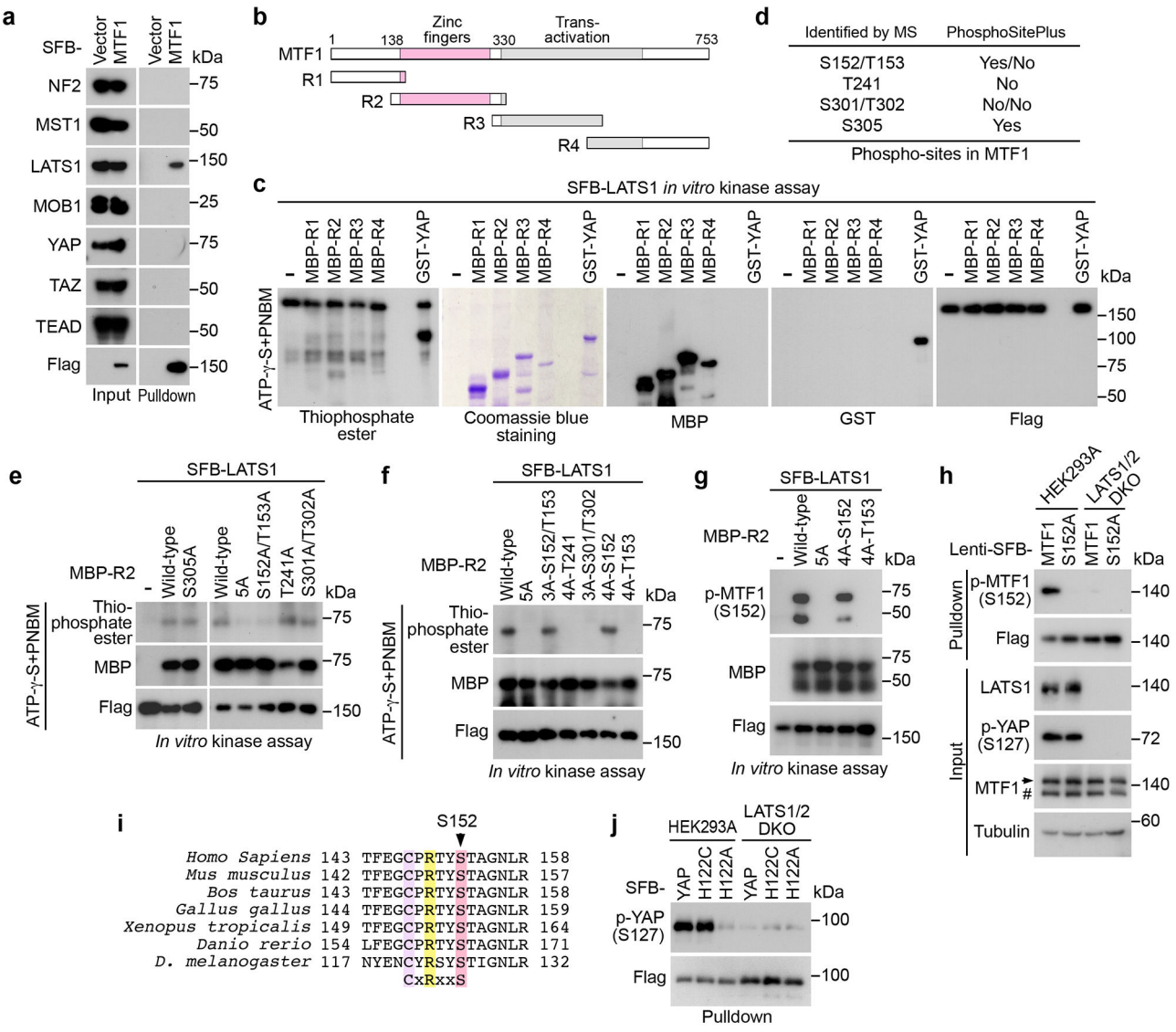

Fig. 4: LATS1 binds and phosphorylates MTF1 at S152.

(**a**) HEK293T cells transfected with SFB-tagged MTF1 construct were subjected to pulldown assay using S protein beads. Western blot was performed using the indicated antibodies.

(**b**) Schematic illustration of MTF1 domains and its truncations.

(**c**) SFB-tagged LATS1 was expressed in HEK293T cells, purified using S protein beads, washed thoroughly with high-salt buffer containing 250 mM NaCl, and subjected to the ATP-γ-S-based *in vitro* kinase assay using the bacterially purified MBP-tagged MTF1-R1/2/3/4 regions (**b**) and GST-YAP as substrates. Western blot was performed using the indicated antibodies.

(**d**) MBP-tagged MTF1-R2 protein was purified from bacteria, used as substrate in the SFB-LATS1 *in vitro* kinase assay, and subjected to mass spectrometry analysis. The identified phosphorylation sites and their PhosphoSite information (https://www.phosphosite.org/) were shown.

(**e-h**) SFB-tagged LATS1 was expressed in HEK293T cells, purified using S protein beads, washed thoroughly with high-salt buffer containing 250 mM NaCl, and subjected to the ATP-γ-S-based *in vitro* kinase assay using the indicated bacterially purified MBP-MTF1-R2 and its mutant proteins as substrates (**e-f**). MTF1-R2-5A represents the MTF1-R2-S152A/T153A/T241A/S301A/T302A mutant. LATS1-induced MTF1-R2 phosphorylation at S152 was validated using anti-phospho-MTF1 S152 antibody via *in vitro* kinase assay (**g**). SFB-tagged MTF1 and its S152A mutant were expressed in wild-type and the LATS1/2 DKO HEK293A cells and purified using S protein beads (**h**). Western blot was performed using the indicated antibodies.

(**i**) Protein sequence alignment shows that MTF1 S152 site is highly conserved among different species. The conserved Cys, Arg and Ser residues were highlighted in colors.

(**j**) The constructs encoding the indicated SFB-tagged YAP and its mutants were expressed in wild-type and the LATS1/2 DKO HEK293A cells, and subjected to pulldown assay using S beads. Western blot was performed using the indicated antibodies.

Data shown represent 2 independent experiments in **a**, **c-h** and **j**.

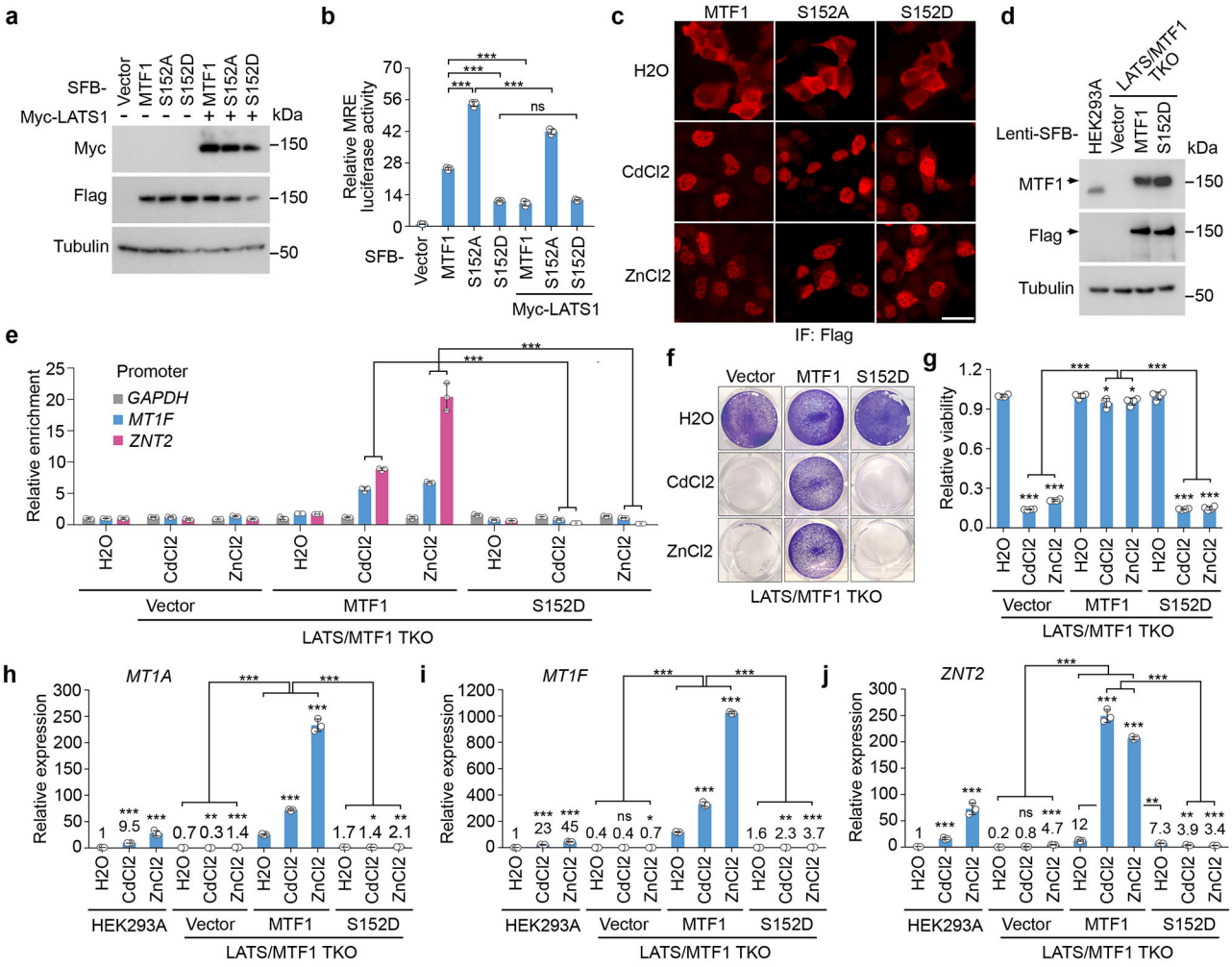

Fig. 5: LATS-mediated MTF1 S152 phosphorylation inhibits heavy metal response.

(**a-b**) HEK293T cells were transfected with the constructs encoding myc-tagged LATS1 and the indicated SFB-tagged MTF1 and its mutants (**a**), and subjected to the MRE luciferase reporter assay (mean ± s.d., n=3 biological replicates) (**b**). *** $p < 0.001$ (two-tailed Student's *t*-test). ns, no significance.

(**c**) HEK293A cells were transfected with the constructs encoding the indicated SFB-tagged MTF1 and its mutants, treated with CdCl2 (50 μM) and ZnCl2 (250 μM) for 1 hour, and subjected to immunofluorescent staining. Scale bar, 40 μm. Data shown represent 3 independent experiments.

(**d**) Wild-type and the LATS/MTF1 TKO HEK293A cells were transduced with the indicated constructs. Western blot was performed using the indicated antibodies. Arrow indicates the exogenously expressed SFB-tagged MTF1 and its S152D mutant.

(**e**) The LATS/MTF1 TKO HEK293A cells were reconstituted with vector and SFB-tagged MTF1 and its S152D mutant, treated with CdCl2 (50 μM) and ZnCl2 (250 μM) for 2 hours, and subjected to ChIP assay. The precipitated DNA was quantified by q-PCR (mean ± s.d., n=3 biological replicates). *** $p < 0.001$ (two-tailed Student's *t*-test).

(**f-g**) The LATS/MTF1 TKO HEK293A cells were reconstituted with vector and SFB-tagged MTF1 and its S152D mutant, treated with CdCl2 (50 μM) and ZnCl2 (250 μM) for 12 hours, visualized by crystal violet staining (**f**), and quantified for relative viability (mean ± s.d., n=4 biological replicates) (**g**). * $p < 0.05$, *** $p < 0.001$ (two-tailed Student's *t*-test).

(**h-j**) The transcription of *MT1A* (**h**), *MT1F* (**i**) and *ZNT2* (**j**) was examined in wild-type and the LATS/MTF1 TKO HEK293A cells reconstituted with vector and SFB-tagged MTF1 and its S152D mutant by q-PCR (mean ± s.d., n=3 biological replicates). Cells were treated with CdCl2 (50 μM) and ZnCl2 (250 μM) for 4 hours. * $p < 0.05$, ** $p < 0.01$, *** $p < 0.001$ (two-tailed Student's *t*-test). ns, no significance.

Data shown represent 2 independent experiments in **a** and **d**.

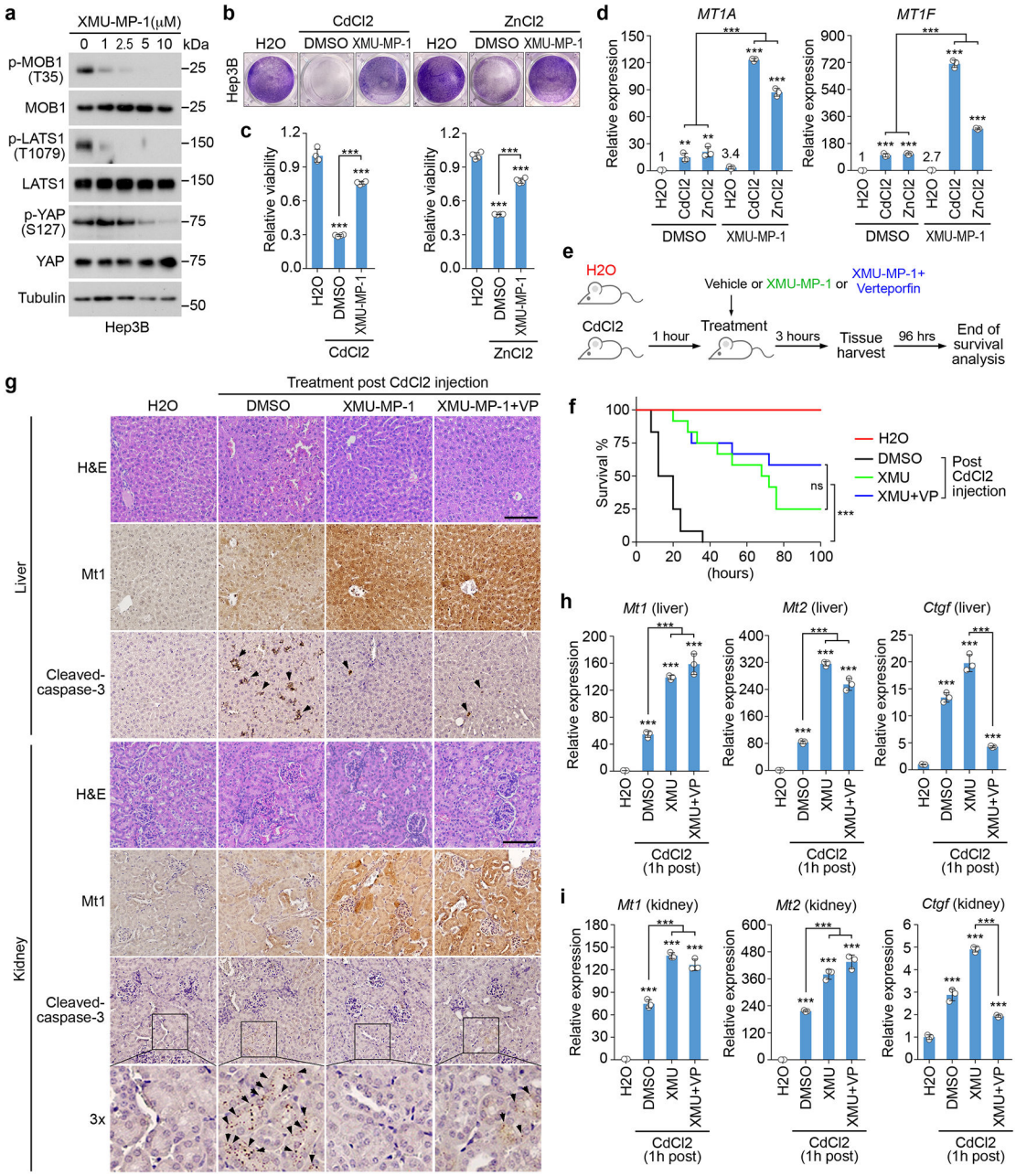

Fig.6: Inhibition of the Hippo pathway promotes heavy metal detoxification.

(**a**) Hep3B cells were treated with XMU-MP-1 at the indicated concentrations for 4 hours. Western blot was performed using the indicated antibodies. Data shown represent 2 independent experiments.

(**b-c**) Hep3B cells were pre-incubated with DMSO and XMU-MP-1 (10 μM) for 4 hours, treated with CdCl2 (50 μM) and ZnCl2 (250 μM) for 12 hours, visualized by crystal violet staining (**b**), and quantified for relative viability (mean ± s.d., n=4 biological replicates) (**c**). *** $p < 0.001$ (two-tailed Student's *t*-test).

(**d**) Hep3B cells were pre-incubated with XMU-MP-1 (10 μM) for 2 hours, and treated with CdCl2 (50 μM) and ZnCl2 (250 μM) for 4 hours. Transcription of *MT1A* and *MT1F* was

examined by q-PCR (mean ± s.d., n=3 biological replicates). ** $p < 0.01$, *** $p < 0.001$ (two-tailed Student's *t*-test).

(**e-i**) Schematic illustration of CdCl2 intoxication experiment in mice was shown (**e**). XMU-MP-1 treatment significantly increased mouse survival upon CdCl2 intoxication (n = 12 mice per group) (**f**). *** $p < 0.001$ (Log-rank test). ns, no significance. Immunohistochemical analyses of Mt1 protein expression and cell apoptosis (cleaved-caspase-3) were performed in the liver and kidney tissues collected from the mice treated with DMSO, XMU-MP-1 alone or combined with VP post CdCl2 intoxication (**g**). H&E, hematoxylin and eosin staining. Arrows indicate the positive cleaved-caspase 3 staining. The indicated regions in the box are shown 3 times enlarged. Scale bar, 150 μM. The transcription of *Mt1*, *Mt2* and *Ctgf* was examined in mouse livers (**h**) and kidneys (**i**) under the indicated treatments by q-PCR (mean ± s.d., n=3 biological replicates). *** $p < 0.001$ (two-tailed Student's *t*-test).

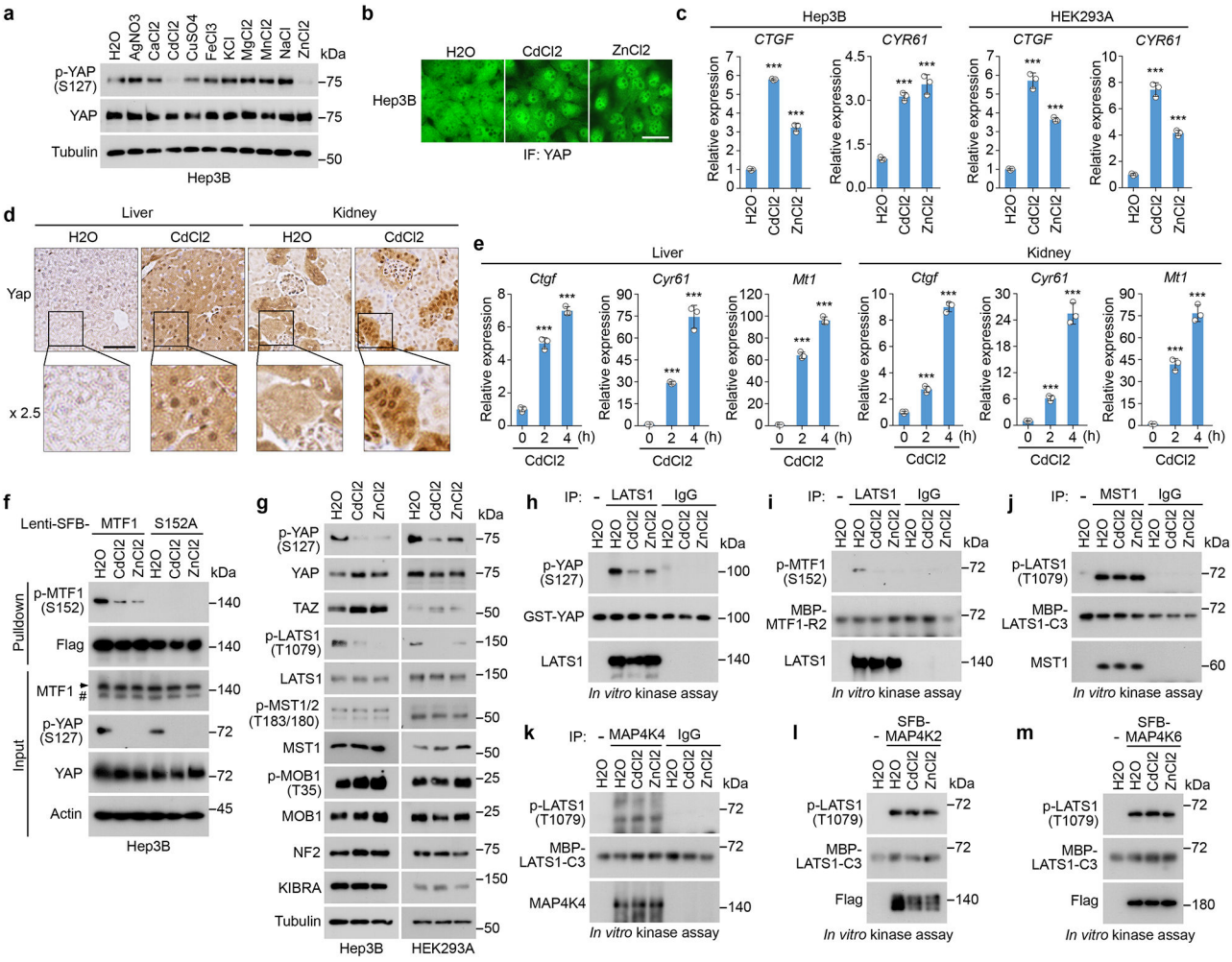

Fig. 7: The Hippo pathway is negatively regulated by heavy metals.

(**a**) Hep3B cells were serum starved for 24 hours and treated with the indicated metals for 1 hour. Western blot was performed using the indicated antibodies. All the metals were used at the concentration of 250 μM except for CdCl2 (50 μM) and AgNO3 (50 μM).

(**b**) Hep3B cells were serum starved for 24 hours, treated with CdCl2 (50 μM) and ZnCl2 (250 μM) for 1 hour, and subjected to immunofluorescent staining. Scale bar, 40 μm. Data shown represent 3 independent experiments.

(**c**) Hep3B and HEK293A cells were serum starved for 24 hours, and treated with CdCl2 (50 μM) and ZnCl2 (250 μM) for 4 hours. The transcription of YAP downstream genes *CTGF* and *CYR61* was examined by q-PCR (mean ± s.d., n = 3 biological replicates). *** $p <$ 0.001 (two-tailed Student's *t*-test).

(**d-e**) Immunohistochemical analysis of Yap was performed in the mouse liver and kidney tissues two hours post CdCl2 treatment (**d**). The indicated regions in the box are shown 2.5 times enlarged. Scale bar, 150 μM. The transcription of genes *Ctgf*, *Cyr61* and *Mt1* was examined at the indicated time points post CdCl2 treatment by q-PCR (mean ± s.d., n=3 biological replicates) (**e**). *** $p < 0.001$ (two-tailed Student's *t*-test).

(**f**) The indicated Hep3B cells were serum starved for 24 hours, treated with CdCl2 (50 μM) and ZnCl2 (250 μM) for 1 hour, and subjected to pulldown assay using S protein beads.
(**g**) Hep3B and HEK293A cells were serum starved for 24 hours, and treated with CdCl2 (50 μM) and ZnCl2 (250 μM) for 1 hour. Western blot was performed using the indicated antibodies.
(**h-m**) Hep3B cells were serum starved for 24 hours, treated with CdCl2 (50 μM) and ZnCl2 (250 μM) for 1 hour, and subjected to immunoprecipitation/pulldown using the indicated antibodies. For LATS1 *in vitro* kinase assay, bacterially purified GST-YAP (**h)** and MBP-MTF1-R2 (**i**) proteins were used as substrates. For MST1 (**j**), MAP4K4 (**k**), SFB-MAP4K2 (**l**) and SFB-MAP4K6 (**m**) *in vitro* kinase assays, bacterially purified MBP-LATS1-C3 protein was used as substrate. Western blot was performed using the indicated antibodies. Data shown represent 2 independent experiments in **a**, **f-m**.

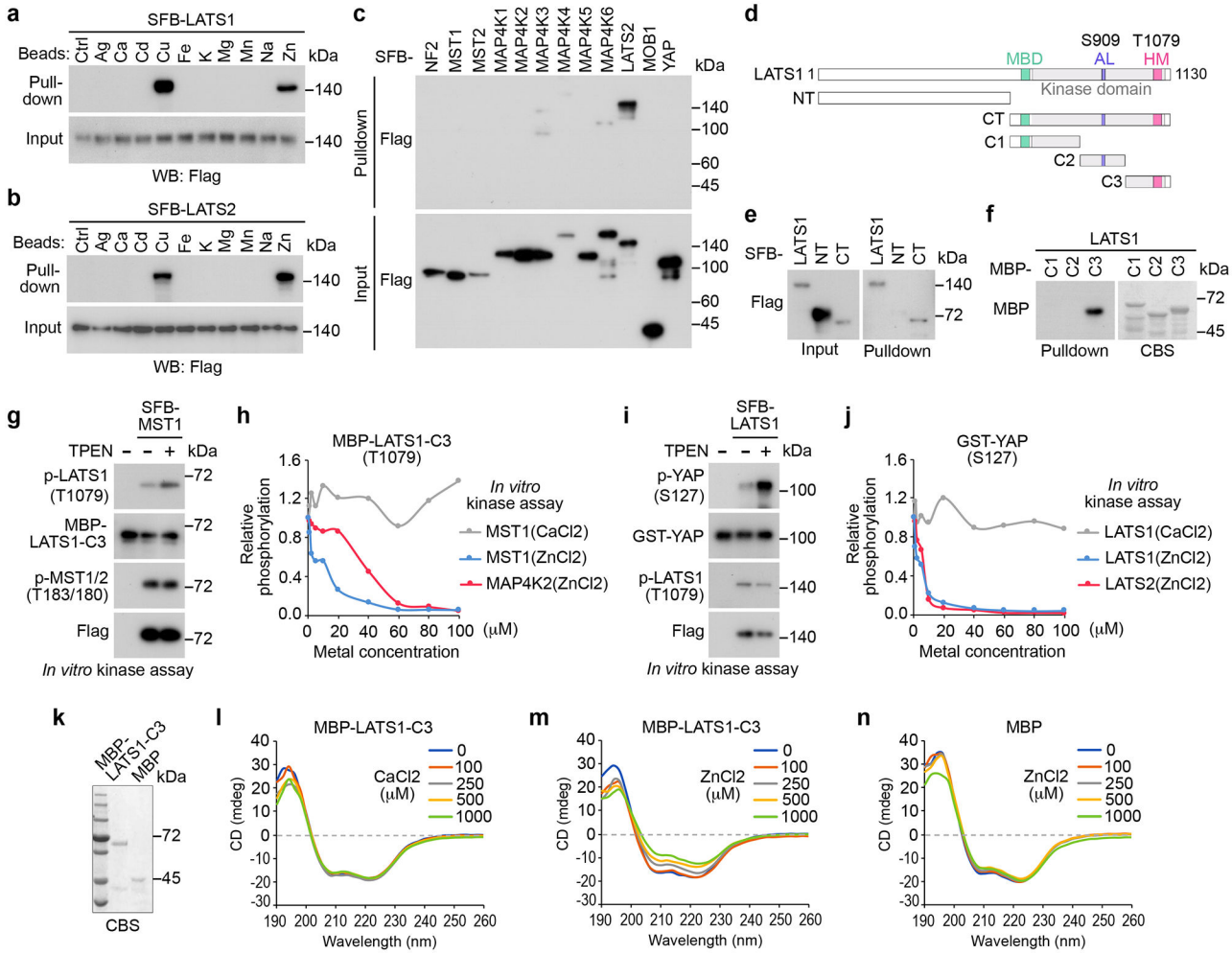

Fig. 8: Zn binds and inhibits LATS.

(**a-b**) HEK293T cells were transfected with the constructs encoding SFB-tagged LATS1 (**a**) and LATS2 (**b**), and subjected to pulldown assay.

(**c**) HEK293T cells were transfected with the constructs encoding the indicated SFB-tagged Hippo pathway components, and subjected to pulldown assay.

(**d**) Schematic illustration of LATS1 protein domains and its truncations.

(**e**) HEK293T cells were transfected with the constructs encoding the indicated SFB-tagged LATS1 and its truncation mutants, and subjected to pulldown assay.

(**f**) The indicated bacterially purified MBP-tagged LATS1 truncation proteins were subjected to pulldown assay. CBS, coomassie blue staining.

(**g**) SFB-tagged MST1 was expressed in HEK293T cells, purified using S protein beads, washed thoroughly with high-salt buffer containing 250 mM NaCl, and subjected to *in vitro* kinase assay. Bacterially purified MBP-LATS1-C3 protein was incubated with Zn chelator TPEN (25 μM), and used as substrate in the SFB-MST1 *in vitro* kinase assay.

(**h**) SFB-tagged MST1 and MAP4K2 were expressed in HEK293T cells, purified using S protein beads, washed thoroughly with high-salt buffer containing 250 mM NaCl, and subjected to *in vitro* kinase assay using bacterially purified MBP-LATS1-C3 protein as

substrate. The *in vitro* kinase was performed in the presence of Ca and Zn at the indicated concentrations. Relative phosphorylation of MBP-LATS1-C3 at T1079 was shown.
(**i**) SFB-tagged LATS1 was expressed in HEK293T cells, purified using S protein beads, washed thoroughly with high-salt buffer containing 250 mM NaCl, incubated with Zn chelator TPEN (25 μM), and subjected to *in vitro* kinase assay. Bacterially purified GST-YAP protein was used as substrate in the SFB-LATS1 *in vitro* kinase assay.
(**j**) SFB-tagged LATS1 and LATS2 were expressed in HEK293T cells, purified using S protein beads, washed thoroughly with high-salt buffer containing 250 mM NaCl, and subjected to *in vitro* kinase assay using bacterially purified GST-YAP protein as substrate. The *in vitro* kinase was performed in the presence of Ca and Zn at the indicated concentrations. Relative phosphorylation of GST-YAP at S127 was shown.
(**k-n**) MBP (0.2 μg/μL) and MBP-tagged LATS1-C3 (0.2 μg/μL) proteins were purified from bacteria (**k**), incubated with Ca and Zn at the indicated concentrations, and subjected to circular dichroism analysis (**l-n**).
Data shown represent 2 independent experiments in **a-c**, **e-n**.